Synthetic photoswitchable neurotransmitters based on bridged azobenzenes

Gisela Cabré[a,‡], Aida Garrido-Charles[b,‡], Àngels González-Lafont[a,c], Widukind Moormann[d], Daniel Langbehn[d], David Egea[a], José M. Lluch[a,c], Rainer Herges[d], Ramon Alibés[a], Félix Busqué[a], Pau Gorostiza[b,e,f,*] and Jordi Hernando[a,*]

[a] Departament de Química, Universitat Autònoma de Barcelona (UAB), Cerdanyola del Vallès, Spain.

[b] Institut de Bioenginyeria de Catalunya (IBEC), Barcelona Institute of Science and Technology (BIST), Barcelona, Spain.

[c] Institut de Biotecnologia i de Biomedicina (IBB), UAB, Cerdanyola del Vallès, Spain.

[d] Otto Diels-Institute of Organic Chemistry, Christian Albrechts University Kiel, Kiel, Germany.

[e] Institució Catalana de Recerca i Estudis Avançats (ICREA), Barcelona, Spain.

[f] Centro de Investigación Biomédica en Red en Bioingeniería, Biomateriales y Nanomedicina, Zaragoza, Spain.

Supporting Information Placeholder

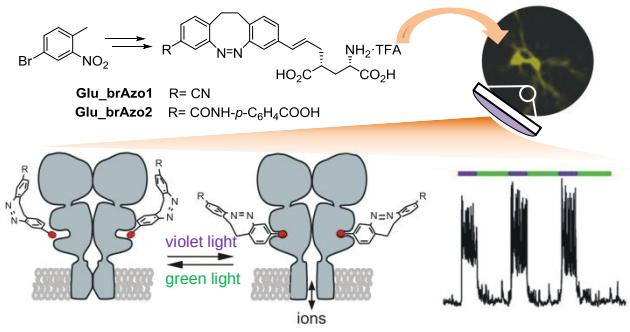

ABSTRACT: Photoswitchable neurotransmitters of ionotropic kainate receptors were synthesized by tethering a glutamate moiety to disubstituted C2-bridged azobenzenes, which were prepared through a novel methodology that allows access to diazocines with higher yields and versatility. Because of the singular properties of these photochromes, photoisomerizable compounds were obtained with larger thermal stability for their inert *cis* isomer than for their biologically activity *trans* state. This enabled selective neuronal firing upon irradiation without background activity in the dark.

By enabling remote manipulation of neuronal signaling with light, optogenetics[1] and photopharmacology[2] have revolutionized neuroscience and neurobiology. Neural receptors responding to glutamate (GluRs), the primary excitatory neurotransmitter, are one of the major targets in these fields, since they regulate several key processes in the nervous system and are related to numerous diseases.[3] As such, a plethora of photopharmacological tools have been developed for light-gating GluRs,[4] among which photochromic ligands (PCLs)[5-12] are often preferred because they combine (a) the advantages of small-molecule, freely diffusing drugs with (b) the capacity for reversibly photoswitching their activity without by-product generation nor modification of native receptors.[2,4]

The major strategy employed to derive PCLs relies on introducing an azoaromatic photoswitch into the structure of well-known, biologically-active ligands.[2,4] Upon *trans-cis* photoisomerization,[13] a geometrical change is induced in these compounds that alters their interaction with the receptor. Typically, the more extended configuration of the *trans* isomer favors such interaction, while affinity is reduced for the folded *cis* state due to steric effects (i.e. *trans*-active PCLs).[2,4] Because of the inherent photochemical properties of azo-aromatic compounds,[13] this imposes a severe limitation to most PCLs developed to date for GluRs[5-11] (and other receptors2): they are active in the dark, where they lie in the more stable *trans* state. Consequently, these compounds elicit strong tonic responses in the absence of illumination (e.g. when acting as receptor agonists), which drastically hampers their use. This is the case of **GluAzo** (Figure 1a), which is a *trans*-active, *trans*-stable partial agonist of ionotropic kainate receptors GluK1 and GluK2,[5,14,15] two of the principal GluRs mediating excitatory neurotransmission in the central nervous system.[3]

To overcome this obstacle while preserving the main design principles behind azo-based PCLs, bridged azobenzenes (brAzo) such as diazocines (C2 bridge, Figure 1b) could be used as photochromes, since they (a) should also favor *trans*-active behavior by switching between extended *trans* and bent *cis* configurations, but (b) exhibit *cis* thermal stability.[16-23] This combination of properties should therefore allow direct administration of the inert *cis* form of the PCL, which could then be selectively photoactivated. In addition, diazocines isomerize with visible light,[16-23] which is a further advantage with respect to common UV-responding azoaromatic compounds.[13] However, the limited synthetic accessibility and versatility of these photochromes has so far limited their application to the photocontrol of biological systems.[22,23b] Actually, their use in photopharmacology to modulate the activity of *N*-methyl-D-aspartate (NMDA) receptors and potassium ion channels has only been reported very recently,[24] for which a low-yield 4-mono-substituted diazocine previously described was employed.[23]

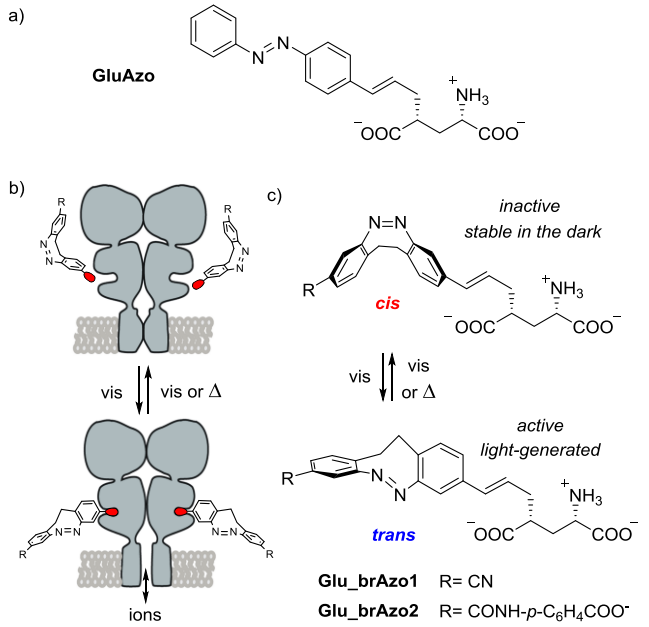

Figure 1. (a) Structure of **GluAzo**.5 (b) Strategy proposed to prepare *trans*-active, *cis*-stable PCLs based on C2-bridged azobenzenes for the light-control of neuronal membrane receptors GluK1 and GluK2. (b) Photoisomerization of **Glu_brAzo1-2**.

In this work we aim to apply this strategy to photocontrol GluK1 and GluK2, while broadening its scope by developing diazocine-based PCLs with larger yields and multiple functionalization sites to favor chemical versatility. To reach this goal our attention focused on 3,3'-disubstituted diazocines,[17,18,21] because very inefficient syntheses have been reported to date for 4,4'-disubstituted analogues (< 1% yield[22]). Based on these photochromes and the structure of **GluAzo**,[5] we designed **Glu_brAzo2** as the first *trans*-active, *cis*-stable agonist of GluK1 and GluK2 by tethering a diazocine unit to a biologically active glutamate moiety through a vinyl linker (Figure 1c). In addition, we took advantage of the disubstitution pattern of the photochrome to introduce a lateral ionic, bulky group for (a) enhancing solubility in aqueous media, and (b) further hindering the interaction of the *cis* isomer with the receptor by increasing the steric congestion around the glutamate moiety. The latter should boost the difference in activity between the two states of the PCL, a required feature given the moderate photoconversions of most functionalized diazocines.[17,18,20-23] To evaluate this effect, **Glu_brAzo1** lacking the additional bulky substituent was also synthesized (Figure 1c).

To validate our design principles, we conducted molecular docking simulations for the two isomers of **Glu_brAzo1-2** on kainate receptors. Our attention particularly focused on GluK2, since (a) it presents a narrower binding cavity that imposes larger steric constraints to ligands,[25] and (b) the crystallographic structure of its ligand-binding domain after complexation with *trans*-**GluAzo** is available.[15] Dockings were computed on this structure keeping the protein rigid, while the initial geometries of the PCLs were optimized at the B3LYP/6-31G(d) level. In all the cases, the best docking solutions placed the glutamate moiety of the ligands in a very similar position as with *trans*-**GluAzo**,[26] thus suggesting analogous interaction with the receptor via hydrogen bonds. However, clear differences were observed for the binding arrangement of each ligand (Figure 2 and S1), which led to different complexation energies (in Chemscore units[27]): 41.2, 37.0, 48.0, 37.3 for *trans*-**Glu_brAzo1**, *cis*-**Glu_brAzo1**, *trans*-**Glu_brAzo2** and *cis*-**Glu_brAzo2** respectively. Importantly, these figures indicate larger affinity of the *trans* isomers of **Glu_brAzo1-2** to GluK2, thus preserving the targeted *trans*-active behavior of **GluAzo**. By contrast, they do not support our hypothesis that the introduction of an ionic, bulky group in **Glu_brAzo2** should decrease the binding efficiency of the *cis* isomer with respect to less hindered **Glu_brAzo1**. It must be noted, however, that this is compensated by the higher complexation energy calculated for *trans*-**Glu_brAzo2** relative to *trans*-**Glu_brAzo1**, which arises from the additional attractive hydrogen bonding and lipophilic interactions formed between its bulky group and the receptor. Therefore, an enhanced contrast in biological activity is indeed to be expected between the two states of **Glu_brAzo2**, as originally designed.

Based on our experience in the synthesis of C2-bridged azobenzenes[16-21] and light-responsive glutamate ligands,[28-30] we devised a linear sequence to prepare **Glu_brAzo1-2** by Heck coupling reaction between their constituting units: a 3,3'-disubstituted diazocine and previously reported, protected glutamate derivative **1**[29] (Scheme 1). The preparation of the photochromic unit started from commercially available 4-bromo-2-nitrotoluene, **3**, which was subjected to deprotonation with potassium *tert*-butoxide and further oxidation with bromine to afford dinitro derivative **4**. When attempting common reductive ring-closing conditions on this intermediate that had been previously reported for the synthesis of diazocines (e.g. Zn, $Ba(OH)_2$),[16-21] formation of the desired bridged azobenzene was only observed with very low yields (< 14%). This prompted us to develop a new methodology for the azocyclization process, for which we explored Mills coupling reaction. With this aim, we first reduced the nitro groups of **4** using sodium sulphide,[31] which delivered diamine **5** in 90% yield. Then, oxidative coupling of **5** was undertaken in the presence of Oxone®[32] in glacial acetic acid[33] at room temperature for 1 h, which nicely furnished dibromosubstituted diazocine **6** in good yield (40%). According to this result, Oxone®-mediated oxidation of one of the aniline moieties to provide the corresponding nitrosoarene followed by condensation with the other, unaltered aniline emerges as a novel one-pot synthesis of diazocines with reproducible yields.

Azobenzene **6** was next monocyanated under standard Rosenmund-von Braun conditions[34] to obtain common asymmetric diazocine **7** in 78% yield (based on recovered **6**). This

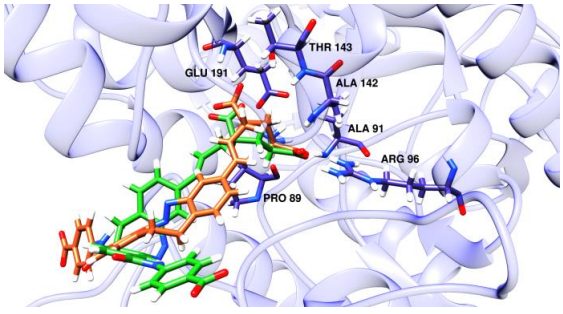

Figure 2. Best docking solutions for *trans*-**Glu_brAzo2** (orange) and *cis*-**Glu_brAzo2** (green) in GluK2. The protein residues interacting with the glutamate group of both ligands are also indicated. Oxygen, nitrogen and hydrogen atoms are depicted in red, blue and white, respectively.

Scheme 1. Synthesis of Glu_brAzo1 and Glu_brAzo2

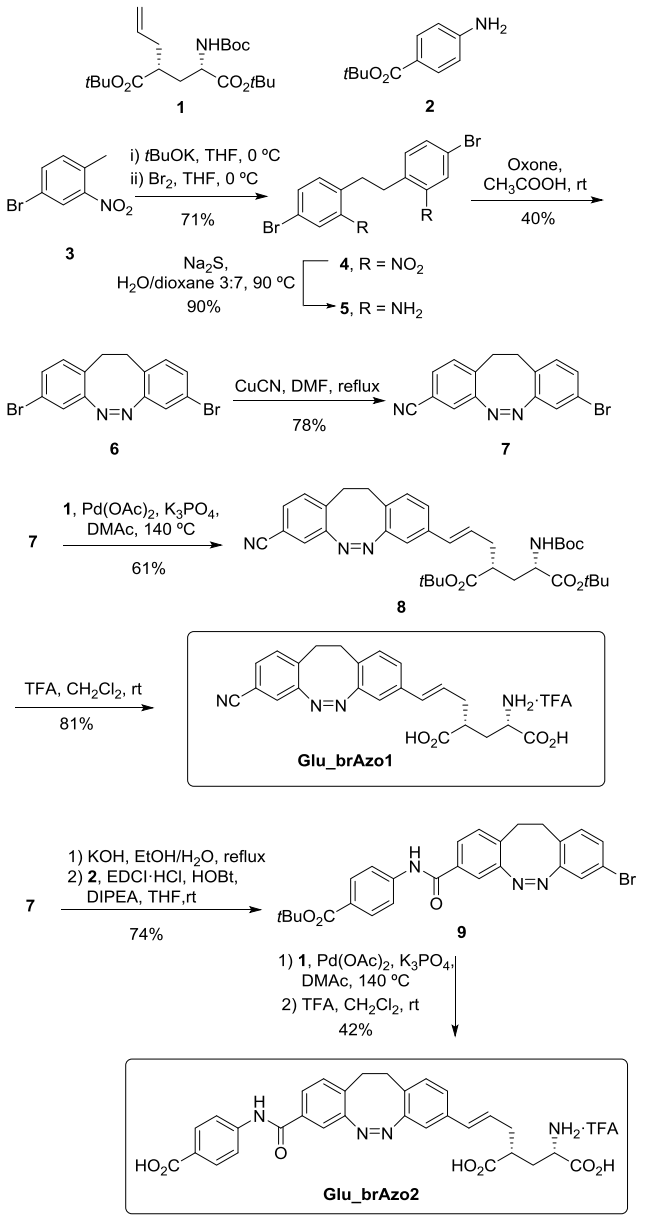

compound was directly coupled to glutamate **1** under Palladium catalysis, for which proper selection of the base and the solvent was found to be fundamental. After several tests, the reaction was performed with K_3PO_4 and *N*,*N*-dimethylacetamide[3,5] at 140 °C under argon in the presence of 0.1 mol% $Pd(OAc)_2$, which delivered **8** in 61% yield. Finally, acid removal of the protecting groups gave the target compound **Glu_brAzo1** as its monotrifluoroacetate salt in good yield. For **Glu_brAzo2**, intermediate **7** was hydrolyzed in basic medium to give the corresponding acid, which was then tethered to previously prepared amine **2** using carbodiimide coupling reagent EDCI·HCl along with HOBt to afford **9** in 74% yield for the two steps. Heck reaction of this compound with **1** under the aforementioned conditions and subsequent removal of the protecting groups finally delivered the target PCL. It must be noted that, despite its larger structural complexity, **Glu_brAzo2** was obtained with an overall yield that is ca. 2- to 10-fold larger than those recently reported for diazocine-based PCLs,[24] thus paving the way for the general application of this strategy in photopharmacology.

By comparison with previous data reported for diazocines,[16-21] NMR and UV-vis absorption analysis confirmed obtainment of the *cis* isomer of **Glu_brAzo1-2** due to their larger stability. In addition, upon irradiation of their n-π^* absorption band with violet light ($\lambda_{abs,max} \sim 395$ nm, $\lambda_{exc} = 405$ nm), spectral changes were observed indicative of *cis-trans* isomerization (Figures 3a and S2-S4). This is the case of the new red-shifted absorption band found at $\lambda_{abs,max} \sim 480$ nm, which is distinctive of the *trans* isomer of diazocines[16-18,20-23] and allowed reverting the isomerization process by green light illumination (λ_{exc} = 532 nm, Figure 3a and S2-S3 and S5). Further characterization of **Glu_brAzo1-2** revealed that they undergo *cis-trans* photoisomerization with moderate quantum yields ($\Phi_{cis\text{-}trans} \sim 0.1$) and efficiencies in aqueous media (Table S1), which resulted in photostationary state mixtures ($PSS_{cis\text{-}trans}$) containing 47% and 60% of their *trans* isomer, respectively. By contrast, *trans-cis* photoconversion proceeded quantitatively with high quantum yields ($\Phi_{trans\text{-}cis} \sim 0.9$), thus ensuring fast light-induced recovery of *cis*-**Glu_brAzo1-2** (Table S1) and repetitive photoswitching without degradation (Figure S6). Back-isomerization of the *trans* state of these compounds was also found to occur in the dark, though at a very much longer time scale ($t_{1/2} \sim 4$ h at 298 K in aqueous media, Figure S7 and Table S1).

To assess the capacity of **Glu_brAzo1-2** to light-gate GluRs, whole-cell voltage clamp recordings were conducted on HEK293 cells expressing GluK1 or GluK2, whose activation causes channel opening and ion flux across the membrane (Figure 1b).[3,5] After perfusion of **Glu_brAzo1-2**, clear changes in the currents evoked in these cells were observed upon irradiation, which were consistent with the different absorption properties of their *cis* and *trans* isomers (Figure 3b and S8-S10). In particular, maximal inward currents arising from

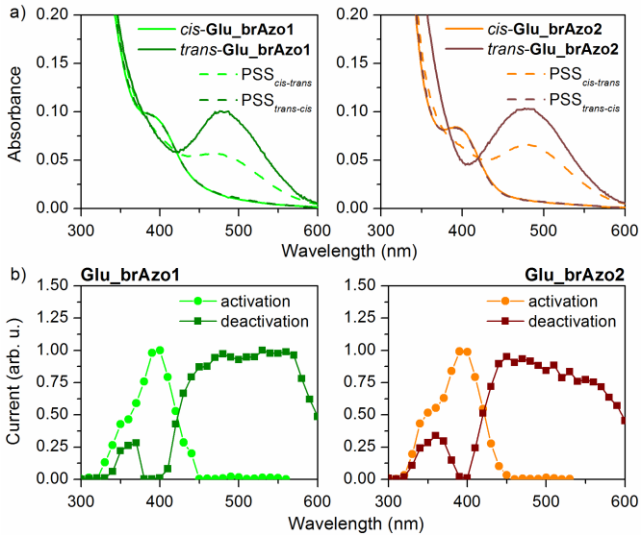

Figure 3. (a) Absorption spectra of both isomers of **Glu_brAzo1** and **Glu_brAzo2** in PBS:DMSO 1:1, as well as of the PSS mixtures obtained under *cis-trans* (λ_{exc} = 405 nm) and *trans-cis* (λ_{exc} = 532 nm) photoisomerization. (b) Activation and deactivation spectra of GluK2 in HEK293 cells after perfusion of **Glu_brAzo1** or **Glu_brAzo2** and irradiation to induce *cis-trans* (for activation) and *trans-cis* (for deactivation) photoisomerization.

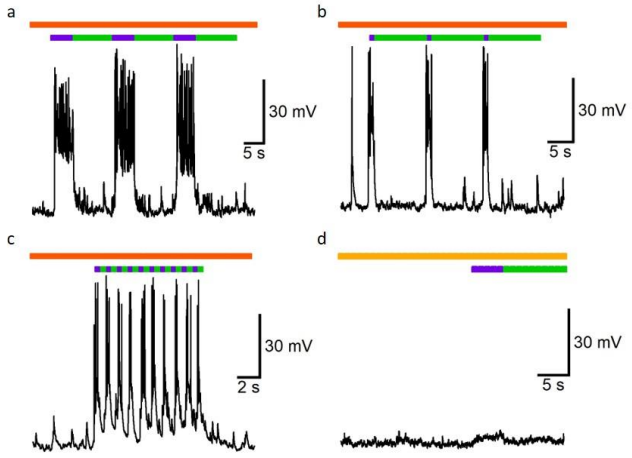

Figure 4. Whole-cell current clamp recordings of rat hippocampal neurons in culture after perfusion of **Glu_brAzo2** (30 μM) and irradiation at λ_{exc} = 390 (purple) and 530 nm (green). Successful neuron activation was observed with 390 nm light pulses of (a) 5 s, (b) 1s, and (c) 0.5 s (1 Hz stimulation), while it was inhibited upon perfusion of DNQX (10 μM). Neurons were current clamped at -60 mV and, to truly report on their GluK2-mediated gating and connectivity, no Concanavalin A was used to prevent receptor desensitization after activation.

receptor activation were measured at λ_{exc} = 390-400 nm (i.e. when inducing *cis*-*trans* photoisomerization of the PCLs). Minimal signals due to receptor deactivation were instead detected in the dark (i.e. for *cis*-**Glu_brAzo1-2**) and at λ_{exc} > 450 nm (i.e. upon *trans*-*cis* photoisomerization). As predicted by our molecular docking calculations, preferential interaction between the glutamate agonist ligand and GluK1/GluK2 was therefore observed for the *trans* state of **Glu_brAzo1-2**, which allowed light-induced manipulation of these receptors.

The *trans*-active behavior of **Glu_brAzo1-2** was further demonstrated when measuring their dose-response curves with GluK1 and GluK2 in the dark and at λ_{exc} = 390 (10-300 μM, Figure S11). In all the cases, larger inward current signals were retrieved for the $PSS_{cis\text{-}trans}$ mixture generated upon irradiation of the initial *cis* isomer, though with (a) low-to-moderate photoinduced modulation (*ca*. 10-35% current increase with respect to the dark) and (b) maximal values that were only about 20-40% of those evoked by free glutamate at 300 μM. Three main factors should account for these results: incomplete photoconversion into the active *trans* isomer, as observed in solution (< 60%, Table S1); limited modification of the glutamate-binding site affinity upon *cis*-*trans* isomerization; and the steric effects imparted by the appended diazocine group with respect to free glutamate even in its less-hindered *trans* configuration, which are of especial importance for GluK2 interaction owing to its narrower ligand binding cavity.[25] Actually, the latter accounts for the lower inward current signals with higher light-induced selectivity obtained for this receptor. However, it did not prevent **Glu_brAzo2** bearing a bulkier terminal group to (a) show higher activity (*ca*. 2-fold increase with respect to **Glu_brAzo1** for GluK2), as anticipated by our molecular docking simulations, which (b) is further modulated upon photoisomerization, as pursued in our initial design.

Glu_brAzo1-2 were finally tested as photoswitchable neurotransmitters in hippocampal neurons where GluK2 is highly expressed.[36] Because of their *trans*-active, *cis*-stable behavior, physiological behavior was not altered upon perfusion of **Glu_brAzo1-2** in the dark, a clear advantage over most PCLs reported for GluRs to date such as **GluAzo**.[5-11] Neuronal firing was instead selectively induced upon *cis*-*trans* photoisomerization of **Glu_brAzo2** at relatively low concentrations (30 μM, Figure 4a-c) and weak light intensities (22.0 and 47.4 μW mm^{-2} at λ_{exc} = 390 and 530 nm, respectively). As a result, sequential and sustained trains of action potentials could be triggered with **Glu_brAzo2** by consecutively switching between violet and green light illumination, even at low irradiation powers and high excitation frequencies (up to 1 Hz, Figure 4c). Interestingly, this photoinduced behavior was inhibited by addition of DNQX,[37] a well-known antagonist of kainate and AMPA GluRs (Figure 4d), which further demonstrates that the efficient photoactivation of hippocampal neurons accomplished with **Glu_brAzo2** arose from its light-dependent interaction with GluK2. Noticeably, this clean physiological effect was achieved despite the limited activity modulation measured upon **Glu_brAzo2** photoisomerization in GluK2-expressing HEK293 cells (*ca.* 20% at 30 μM concentration), while it could not be reproduced with the slightly less efficient **Glu_brAzo1** agonist (Figure S12). We ascribe this situation to the well-known nonlinear behavior of neuronal signaling, since ligand interaction with a minimum fraction of glutamate receptors is needed to overcome the depolarization threshold required to initiate an action potential.5 In our case, such threshold was only surpassed with *trans*-**Glu_brAzo2**, probably due to its larger affinity for GluK2, as suggested by our measurements in cultured cells.

In conclusion, we demonstrated in this work the potential of C2-bridged azobenzenes for the preparation of azo-based photochromic ligands capable of light-controlling neural receptors, which preserve the larger activity typically observed for their *trans* state while ensuring larger stability for the inert *cis* isomer. By introducing a novel synthetic methodology for the preparation of 3,3'-disubstituted diazocines based on an Oxone®-mediated intramolecular azocyclization reaction, the desired ligands could be obtained with higher yields and larger versatility, thus enabling fine-tuning of their light-dependent biological response. As a proof of concept, this strategy was applied to the preparation of new photoswitchable neurotransmitters for the light-induced operation of kainate glutamate receptors, with which we achieved selective neural firing upon irradiation without background activity in the dark.

ASSOCIATED CONTENT

Supporting Information

The Supporting Information is available free of charge on the ACS Publications website.

General methods and materials, synthetic procedures, and additional computational, photochemical and electrophysiological data (PDF)

AUTHOR INFORMATION

Corresponding Author

* pau@icrea.cat (P.G.), jordi.hernando@uab.cat (J.H.)

Author Contributions

‡These authors contributed equally.

Notes

The authors declare no competing financial interests.

ACKNOWLEDGMENT

We acknowledge financial support from MINECO/FEDER (projects CTQ2015-65439-R, CTQ2016-80066-R, CTQ2016-75363-R and CTQ2017-83745-P), AGAUR/Generalitat de Catalunya (CERCA Programme and projects 2017-SGR-00465 and 2017-SGR-1442), Human Brain Project WAVESCALES projects, Fundaluce foundation, and Deutsche Forschungsgemeinschaft (SFB677). G. C. acknowledges the Generalitat de Catalunya for her pre-doctoral FI grant. A. G.-C. was supported by fellowship BES-2014-068169.

REFERENCES

(1) (a) Deisseroth, K. *Nat. Methods* **2011**, *8*, 26-29. (b) Deisseroth, K. *Nat. Neurosci.* **2015**, *18*, 1213-1225.

(2) (a) Gorostiza, P; Isacoff, E. Y. *Science* **2008**, *322*, 395-399. (b) Fehrentz, T.; Schonberger, M.; Trauner, D. *Angew. Chem., Int. Ed.* **2011**, *50*, 12156−12182. (c) Kramer, R. H.; Mourot, A.; Adesnik, H. *Nat. Neurosci.* **2013**, *16*, 816−823. (d) Velema, W. A.; Szymanski, W.; Feringa, B. L. *J. Am. Chem. Soc.* **2014**, *136*, 2178−2191. (e) Berlin, S.; Isacoff, E. Y. *EMBO Rep.* **2017**, *18*, 677-692. (f) Hüll, K.; Morstein, J.; Trauner, D. *Chem. Rev.* **2018**, *118*, 10710-10747.

(3) (a) Traynelis, S. F.; Wollmuth, L. P.; McBain, C. J.; Menniti, F. S.; Vance, K. M.; Ogden, K. K.; Hansen, K. B.; Yuan, H.; Myers, S. J.; Dingledine, R. *Pharmacol. Rev.* **2010**, *62*, 405–496. (b) Niswender, C. M.; Conn, P. J. *Annu. Rev. Pharmacol. Toxicol.* **2010**, *50*, 295–322. (c) Bowie, D. *CNS Neurol Disord Drug Targets* **2008**, *7*, 129–143.

(4) Reiner, A.; Levitz, J.; Isacoff, E. Y. *Curr. Opin. Pharmacol*. **2015**, *20*, 135-143.

(5) Volgraf, M.; Gorostiza, P.; Szobota, S.; Helix, M. R.; Isacoff, E. Y.; Trauner, D. *J. Am. Chem. Soc.* **2007**, *129*, 260-261.

(6) Stawski, P.; Sumser, M.; Trauner, D. *Angew. Chem. Int. Ed.* **2012**, *51*, 5748-5751.

(7) Pittolo, S.; Gómez-Santacana, X.; Eckelt, K.; Rovira, X.; Dalton, J.; Goudet, C.; Pin, J. P.; Llobet, A.; Giraldo, J.; Llebaria, A.; Gorostiza, P. *Nat. Chem. Biol.* **2014**, *10*, 813-815.

(8) Rovira, X.; Trapero, A.; Pittolo, S.; Zussy, C.; Faucherre, A.; Jopling, C.; Giraldo, J.; Pin, J.-P.; Gorostiza, P.; Goudet, C.; Llebaria, A. *Cell Chem. Biol.* **2016**, *23*, 929−934.

(9) Barber, D. M.; Liu, S. A.; Gottschling, K.; Sumser, M.; Hollmann, M.; Trauner, D. *Chem. Sci.* **2017**, *8*, 611–615.

(10) Gómez-Santacana, X.; Pittolo, S.; Rovira, X.; Lopez, M.; Zussy, C.; Dalton, J. A. R.; Faucherre, A.; Jopling, C.; Pin, J.-P.; Ciruela, F.; Goudet, C.; Giraldo, J.; Gorostiza, P.; Llebaria, A. *ACS Cent. Sci.* **2017**, *3*, 81-91.

(11) Hartrampf, F. W. W.; Barber, D. M.; Gottshcling, K.; Leippe, P.; Hollmann, M.; Trauner, D. *Tetrahedron* **2017**, *73*, 4905-4912.

(12) Laprell, L.; Repak, E.; Franckevicius, V.; Hartrampf, F.; Terhag, J.; Hollmann, M.; Sumser, M.; Rebola, N.; DiGregorio, D. A.; Trauner, D. *Nat. Commun*. **2015**, *6*, *8076*.

(13) Bandara, H. M. D.; Burdette, S. C. *Chem. Soc. Rev.* **2012**, *41*, 1809-1825.

(14) Abrams, Z. R.; Warrier, A.; Trauner, D.; Zhang, X. *Front. Neural Circuits* **2010**, *4*, 13.

(15) Reiter, A.; Skerra, A.; Trauner, D.; Schiefner, A. *Biochemistry* **2013**, *52*, 8972-8974.

(16) Siewertsen, R.; Neumann, H.; Buchheim-Stehn, B.; Herges, R.; Nather, C.; Renth, F.; Temps, F. *J. Am. Chem. Soc.* **2009**, *131*, 15594−15595.

(17) Sell, H.; Nather, C.; Herges, R. *Beilstein J. Org. Chem.* **2013**, *9*, 1−7.

(18) Tellkamp, T.; Shen, J.; Okamoto, Y.; Herges, R. *Eur. J. Org. Chem.* **2014**, *2014*, 5456−5461.

(19) Hammerich, M.; Schütt, C.; Stahler, C.; Lentes, P.; Rohricht, F.; Höppner, R.; Herges, R. *J. Am. Chem. Soc.* **2016**, *138*, 13111−13114.

(20) Moormann, W.; Langbehn, D.; Herges, R. *Synthesis* **2017**, *49*, 3471-3475.

(21) Moormann, W.; Langbehn, D.; Herges, R. *Beilstein J. Org. Chem.* **2019**, *16*, 727-732.

(22) Samanta, S.; Qin, C. G.; Lough, A. J.; Woolley, G. A. *Angew. Chem. Int. Ed.* **2012**, *51*, 6452−6455.

(23) (a) Joshi, D. K.; Mitchell, M. J.; Bruce, D.; Lough, A. J.; Yan, H. *Tetrahedron* **2012**, *68*, 8670-8676. (b) Eljabu, F.; Dhruval, J.; Yan, H. *Bioorg. Med. Chem. Lett.* **2015**, *25*, 5594-5596; (c) Jun, M.; Joshi, D. K.; Yalagala, R. S.; Vanloon, J.; Simionescu, R.; Lough, A. J.; Gordon, H. L.; Yan, H. *ChemistrySelect* **2018**, *3*, 2697−2701.

(24) Thapaliya, E. R.; Zhao, J.; Ellis-Davies, G. C. R. *ACS Chem. Neurosci.* **2019**, 10.1021/acschemneuro.8b00734.

(25) Mayer, M. L. *Neuron*, **2005**, *45*, 539-552.

(26) Guo, Y.; Wolter, T.; Kubar, T.; Sumser, M.; Trauner, D.; Elstner, M. *PLoS One* **2015**, *10*, e0135399.

(27) Eldridge, M. D.; Murray, C. W.; Auton, T. R.; Paolini, G. V.; Mee, R. P. *J. Comput.-Aided Mol. Des.* **1997**, *11*, 425–445..

(28) Izquierdo-Serra, M.; Gascón-Moya, M.; Hirtz, J. J.; Pittolo, S.; Poskanzer, K. E.; Ferrer, È.; Alibés, R.; Busqué, F.; Yuste, R.; Hernando, J.; Gorostiza, P. *J. Am. Chem. Soc.* **2014**, *136*, 8693-8701.

(29) Gascón-Moya, M.; Pejoan, A.; Izquierdo-Serra, M.; Pittolo, S.; Cabré, G.; Hernando, J.; Alibés, R.; Gorostiza, P.; Busqué, F. *J. Org. Chem.* **2015**, *80*, 9915-9925.

(30) Cabré, G.; Garrido-Charles, A.; Moreno, M.; Bosch, M.; Porta-de-la-Riva, M.; Krieg, M.; Gascón-Moya, M.; Camarero, N.; Gelabert, R.; Lluch, J. M.; Busqué, F.; Hernando, J.; Gorostiza, P.; Alibés, R. *Nat. Commun.* **2019**, *10*, 907.

(31) Mourot, A.; Kienzler, M. A.; Banghart, M. R.; Fehrentz, T.; Huber, F. M. E.; Stein, M.; Kramer, R. H.; Trauner, D. *ACS Chem. Neurosci.* **2011**, *2*, 536–543.

(32) Yu, B. C.; Shirai Y.; Tour, J. M. *Tetrahedron*, **2006**, *62*, 10303-10310.

(33) Davey, H. H.; Lee R. D.; Marks, T. J. *J. Org. Chem.* **1999**, *64*, 4976-4979.

(34) Friedman, L.; Shechter, H. *J. Org. Chem.* **1961**, *26*, 2522-2524.

(35) Yao, Q.; Kinney, E. P.; Yang, Z. *J. Org. Chem.* **2003**, *68*, 7528-7531.

(36) Carta, M.; Fièvre, S.; Gorlewicz, A.; Mulle, C. *Eur. J. Neurosci.* **2014**, *39*, 1835-1844.

(37) Honore, T.; Davies, S. N.; Drejer, J.; Fletcher, E. J.; Jacobsen, P.; Lodge, D.; Nielsen, F. E. *Science* **1988**, *241*, 701-703.

Supporting Information

Synthetic photoswitchable neurotransmitters based on bridged azobenzenes

Gisela Cabré[a,‡], Aida Garrido-Charles[b,‡], Àngels González-Lafont[a,c], Widukind Moormann[d], Daniel Langbehn[d], David Egea,[a] José M. Lluch[a,c], Rainer Herges[d], Ramon Alibés[a], Félix Busqué[a], Pau Gorostiza[b,e,f,*] and Jordi Hernando[a,*]

[a] *Departament de Química, Universitat Autònoma de Barcelona (UAB), Cerdanyola del Vallès, Spain.*

[b] *Institut de Bioenginyeria de Catalunya (IBEC), Barcelona Institute of Science and Technology (BIST), Barcelona, Spain.*

[c] *Institut de Biotecnologia i de Biomedicina (IBB), UAB, Cerdanyola del Vallès, Spain.*

[d] *Otto Diels-Institute of Organic Chemistry, Christian Albrechts University Kiel, Kiel, Germany.*

[e] *Institució Catalana de Recerca i Estudis Avançats (ICREA), Barcelona, Spain.*

[f] *Centro de Investigación Biomédica en Red en Bioingeniería, Biomateriales y Nanomedicina (CIBER-BBN), Zaragoza, Spain.*

[‡] *Equal contribution*

[*] *Corresponding authors: pau@icrea.cat (P. G.), jordi.hernando@uab.cat (J. H.)*

Contents

Experimental procedure for the synthesis of **Glu_brAzo1** and **Glu_brAzo2**	S3
Computational, photochemical and biological supplementary methods	S10
Figure S1. Molecular docking simulations	S14
Figures S2-S7 and Table S1. Photoisomerization of **Glu_brAzo1** and **Glu_brAzo2**	S15
Figure S8-S11. Photomodulation of GluK1 and GluK2 in HEK293 cells using **Glu_brAzo1** and **Glu_brAzo2**	S20
Figure S12. Whole-cell voltage clamp recording of rat hippocampal neurons in culture perfused with **Glu_brAzo1** and **Glu_brAzo2**.	S22
^{1}H and ^{13}C NMR spectra of new compounds	S23
References	S33

Experimental procedure for the synthesis of Glu_brAzo1 and Glu_brAzo2

***General procedure*:** The preparation of ligands **Glu_brAzo1** and **Glu_brAzo2** was achieved via a multistep synthetic sequence (see Scheme 1 in the article). In both cases, we took commercially available 4-bromo-2-nitrotoluene (**3**) as a starting material to form the bridged azobenzene core **6**, to which fully protected glutamate derivative **1** and, in the case of **Glu_brAzo2**, amine **2** were introduced. These fragments were obtained from commercially available products as described in refs. 1 (**1**) and 2 (**2**).

Materials and methods: Commercially available reagents were used as received. Solvents were dried by distillation over the appropriate drying agents. All reactions were monitored by analytical thin-layer chromatography (TLC) using silica gel 60 precoated aluminum plates (0.20 mm thickness). Flash column chromatography was performed using silica gel (230-400 mesh). ^{1}H NMR and ^{13}C NMR spectra were recorded at 250, 360 400 or 500 MHz and 90.5, 100.6 or 125.8 MHz, respectively. Proton chemical shifts are reported in ppm (δ) ($CDCl_3$, δ 7.26 or DMSO-d_6, δ 2.50). Carbon chemical shifts are reported in ppm (δ) ($CDCl_3$, δ 77.16 or DMSO-d_6, δ 39.5). NMR signals were assigned with the help of COSY, HSQC, HMBC and DEPT135. Infrared peaks are reported in cm^{-1}. Melting points were determined on hot stage and are uncorrected. HRMS were recorded using electron ionization (EI) or electrospray ionization (ESI). Optical rotations were measured at 20 ± 3 °C.

Synthesis of* Glu_brAzo1 *and* Glu_brAzo2*: The synthesis of **Glu_brAzo1** and **Glu_brAzo2** proceeded as follows.

1,2-bis(4-bromo-2-nitrophenyl)ethane, 4

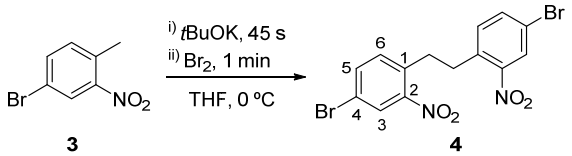

To an ice-cooled solution of 4-bromo-2-nitrotoluene, **3**, (4.00 g, 18.5 mmol) in anhydrous THF (130 mL), *t*BuOK (3.10 g, 27.7 mmol) was added and the solution was stirred for 45 s. Then, Br_2 (1.4 mL, 27.3 mmol) was added and the mixture was stirred for 1 min. The reaction mixture was let warm up to rt and then was poured into ice. The resulting suspension was filtrated and the solid was washed with acetone to furnish **4** (2.84 g, 6.60 mmol, 71%) as an orange solid: mp 219 ºC (from acetone); ^{1}H NMR (500 MHz, $CDCl_3$) δ 8.16 (d, $J_{3,5}$ = 2.1 Hz, 2H, H-3), 7.87 (dd, $J_{5,6}$ = 8.3 Hz, $J_{5,3}$ = 2.1 Hz, 2H, H-5), 7.41 (d, $J_{6,5}$ = 8.3 Hz, 2H, H-6), 3.10 (s, 4H, 2xCH_2); ^{13}C NMR (125.8 MHz,

$CDCl_3$) δ 149.3 (C-2), 134.0 (C-5), 133.9 (C-6), 133.7 (C-1), 126.8 (C-3), 119.6 (C-4), 31.9 (CH_2); IR (ATR) 3088, 1557, 1519, 1473, 1390, 1335 cm^{-1}; MS (EI, 70 eV) *m/z* (%) 213.97 (100) [M^{2+}], 155.97 (66) [M-$C_8H_7BrN_2O_4$]; Anal calcd. for [$C_{14}H_{10}Br_2N_2O_4$]: C, 39.10; H, 2.35; N, 6.51; found: C, 39.17; H, 2.33; N, 6.29. COSY and $^1H/^{13}C$ correlation were recorded.

6,6'-(ethane-1,2-diyl)bis(3-bromoaniline), 5

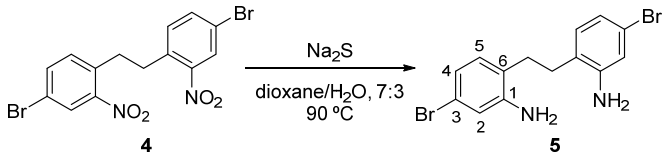

4 **5**

Compound **4** (100 mg, 0.23 mmol) was dissolved in a 7:3 degassed mixture of 1,4-dioxane and water (2.6 ml) under N_2 atmosphere. The reaction mixture was heated to 90 ºC and sodium sulfide (168 mg, 2.15 mmol) was added portion-wise over 2 h. The mixture was stirred overnight. Then, the reaction was quenched with a saturated aqueous solution of $NaHCO_3$ (4 mL) and the crude product was extracted with CH_2Cl_2 (3 x 5 ml). The combined organic layers were washed with H_2O, dried over anhydrous $MgSO_4$ and the solvent was evaporated under vacuum to furnish a crude solid identified as **5** (77 mg, 0.21 mmol, 90% yield): mp 158.8 ºC (from CH_2Cl_2); ^1H NMR (500 MHz, $CDCl_3$) δ 6.84 (m, 4H, H-4, H-5), 6.81 (m, 2H, H-2), 3.63 (br s, 4H, 2x-NH_2), 2.71 (s, 4H, 2xCH_2); ^{13}C NMR (125.8 MHz, $CDCl_3$) δ 145.8 (C-1), 131.1 (C-5), 124.7 (C-6), 121.9 (C-4), 120.7 (C-3), 118.5 (C-2), 30.4 (CH_2); IR (ATR): 3430, 3354, 1619, 1491, 1409, 1179 cm^{-1}; HRMS (HR-EI) calcd. for [$C_{14}H_{14}{}^{79}Br_2N_2$]: 367.9524; found: 367.9525. COSY and $^1H/^{13}C$ correlation were recorded.

(*Z*)-3,8-dibromo-11,12-dihydrodibenzo[*c*,*g*][1,2]diazocine, 6

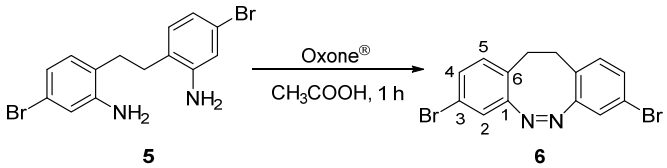

5 **6**

To a solution of **5** (204 mg, 0.55 mmol) in 150 mL glacial acetic acid was added Oxone® (126 mg, 0.83 mmol) in portions. The mixture was stirred at room temperature for 1 h. The solvent was evaporated under reduced pressure. The residue was dissolved in CH_2Cl_2 (25 mL) and washed with saturated $NaHCO_3$ solution (30 mL) and saturated NaCl solution (30 mL). The organic layer was dried over anhydrous $MgSO_4$ and the solvent was evaporated in vacuo. The crude product was purified by column

chromatography (from cyclohexane/ethyl acetate 10% to ethyl acetate 100%) to give **6** as a yellow solid (80 mg, 0.22 mmol, 40% yield).: mp 179 ºC (from EtOAc); ^{1}H NMR (500 MHz, $CDCl_3$) δ 7.16 (dd, $J_{4,5}$ = 8.2 Hz, $J_{4,2}$ = 2.0 Hz, 2H, H-4), 7.00 (d, $J_{2,4}$ = 2.0 Hz, 2H, H-2), 6.86 (d, $J_{5,4}$ = 8.2 Hz, 2H, H-5), 2.82 (m, 4H, 2xCH_2); ^{13}C NMR (125.8 MHz, $CDCl_3$) δ 155.9 (C-1), 131.2 (C-5), 130.4 (C-4), 126.8 (C-6), 121.3 (C-2), 120.3 (C-3), 31.0 (CH_2); IR (ATR) 3042, 2162, 2046, 1743, 1585, 1559, 1465, 1382 cm^{-1}; MS (EI, 70 eV) *m/z* (%) = 365.92 (6) [M$^+$], 257.99 (14) [M-BrN_2], 205.08 (3) [M-Br_2], 178.03 (100) [M-Br_2N_2]; HRMS (EI) calcd. for [$C_{14}H_{10}{}^{79}Br_2N_2$]$^+$: 363.9211; found: 363.9201; Anal calcd. for [$C_{14}H_{10}Br_2N_2$]: C, 45.94; H, 2.75; N, 7.65; found: C, 45.83; H, 2.80; N, 7.50. COSY and ^{1}H/^{13}C correlation were recorded.

(*Z*)-8-bromo-11,12-dihydrodibenzo[*c*,*g*][1,2]diazocine-3-carbonitrile, 7

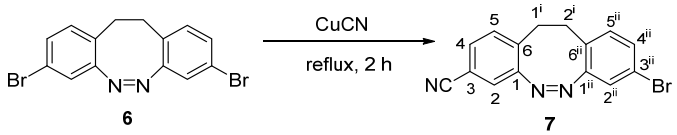

To a solution of **6** (600 mg, 1.64 mmol) in dry DMF (4 mL), CuCN (147 mg, 1.64 mmol) was added. The reaction mixture was stirred for 2 h under reflux conditions. Then, it was let cool down to rt and a 10% aqueous solution of ethylendiamine (45 mL) was added. The product was extracted with CH_2Cl_2 (3 x 50 mL). The combined organic extracts were washed with H_2O (2 x 50 mL), dried over anhydrous $MgSO_4$ and concentrated under vacuum. The resulting residue was purified by column chromatography (cyclohexane/EtOAc, 3:1) to furnish unreacted **6** (210 mg, 0.57 mmol, 35%) and compound **7** (260 mg, 0.83 mmol, 51% yield, 78% yield considering recovered **6**) as a yellow solid. Compound **7**: Mp 179.3 ºC (from EtOAc); ^{1}H NMR (500 MHz, $CDCl_3$) δ 7.34 (dd, $J_{4,5}$ = 7.9 Hz, $J_{4,2}$ = 1.6 Hz, 1H, H-4), 7.18 (dd, $J_{4^{ii},5^{ii}}$ = 8.2 Hz, $J_{4^{ii},2^{ii}}$ = 2.0 Hz, 1H, H-4^{ii}), 7.14 (d, $J_{2,4}$ = 1.6 Hz, 1H, H-2), 7.12 (d, $J_{5,4}$ = 7.9 Hz, 1H, H-5), 7.02 (d, $J_{2^{ii},4^{ii}}$ = 2.0 Hz, 1H, H-2^{ii}), 6.87 (d, $J_{5^{ii},4^{ii}}$ = 8.2 Hz, 1H, H-5^{ii}), 2.90 (m, 4H, H-1^{i}, H-2^{i}); ^{13}C NMR (125.8 MHz, $CDCl_3$) δ 155.8 (C-1^{ii}), 155.1 (C-1), 133.6 (C-6), 131.3 (C-5^{ii}), 130.9 (C-4), 130.7 (C-5), 130.7 (C-4^{ii}), 126.2 (C-6^{ii}), 122.5 (C-2), 121.7 (C-2^{ii}), 120.6 (C-3^{ii}), 117.9 (CN), 111.2 (C-3), 31.7 (C-1^{i}), 30.8 (C-2^{i}); IR (ATR) 3045, 2922, 2231, 1587, 1471 cm^{-1}; HRMS (HR-EI) calcd. for [$C_{15}H_{10}{}^{79}BrN_3$]: 311.0058; found: 311.0056; calcd. for [$C_{15}H_{10}{}^{81}BrN_3$]: 313.00361; found: 313.00361. COSY and ^{1}H/^{13}C correlation were recorded.

di-*tert*-butyl (2*S*,4*R*)-2-((*tert*-butoxycarbonyl)amino)-4-((*E*)-3-((*Z*)-8-cyano-11,12-dihydrodibenzo[*c*,*g*][1,2]diazocin-3-yl)allyl)pentanedioate, 8

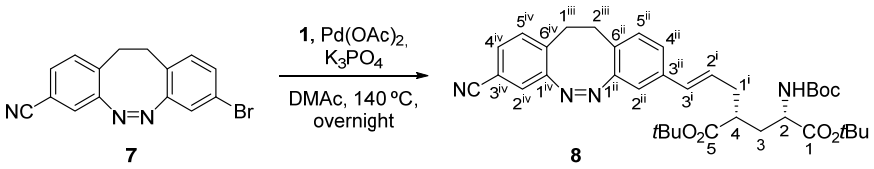

7 **8**

A mixture of diazocine **7** (30 mg, 96 μmol), glutamate derivative **1** (46 mg, 0.12 mmol), $Pd(OAc)_2$ (3 mg, 10 μmol) and K_3PO_4 (30 mg, 0.14 mmol) in DMAc (0.5 mL) under argon atmosphere was heated at 140 ºC overnight. Then, the solvent was evaporated and the resulting residue was purified by column chromatography (hexane/EtOAc, 3:1) to give **8** (37 mg, 59 μmol, 61% yield) as a yellow solid: mp 66.5 ºC (from EtOAc); $[\alpha]_D^{20}$ 14.4 (*c* 1.0, $CHCl_3$); ^{1}H NMR (500 MHz, $CDCl_3$) δ 7.30 (dd, $J_{4^{iv},5^{iv}}$ = 7.9 Hz, $J_{4^{iv},2^{iv}}$ = 1.7 Hz, 1H, H-4^{iv}), 7.11 (d, $J_{5^{iv},4^{iv}}$ = 7.9 Hz, 1H, H-5^{iv}), 7.09 (d, $J_{2^{iv},4^{iv}}$ = 1.7 Hz, 1H, H-2^{iv}), 7.00 (d, $J_{4^{ii},5^{ii}}$ = 8.0 Hz, 1H, H-4^{ii}), 6.89 (d, $J_{5^{ii},4^{ii}}$ = 8.0 Hz, 1H, H-5^{ii}), 6.87 (s, 1H, H-2^{ii}), 6.29 (d, $J_{3^{i},2^{i}}$ = 15.8 Hz, 1H, H-3^{i}), 6.07 (m, 1H, H-2^{i}), 4.99 (d, $J_{NHBoc,2}$ = 8.5 Hz, 1H, NHBoc), 4.23 (m, 1H, H-2), 2.90 (m, 4H, H-1^{iii}, H-2^{iii}), 2.44 (m, 2H, H-1^{i}, H-4), 2.35 (m, 1H, H-1^{i}), 2.15 (m, 1H, H-3), 1.68 (m, 1H, H-3), 1.44 (s, 9H, $C(CH_3)_3$), 1.43 (s, 9H, $C(CH_3)_3$), 1.40 (s, 9H, $C(CH_3)_3$); ^{13}C NMR (125.8 MHz, $CDCl_3$) δ 173.9 (C-5), 171.7 (C-1), 155.6 (C-1^{ii}), 155.1 (C-1^{iv}), 136.7 (C-3^{ii}), 134.3 (C-6^{iv}), 130.8 (C-3^{i}, C-5^{iv}), 130.7 (C-4^{iv}), 130.2 (C-5^{ii}), 128.2 (C-2^{i}), 126.0 (C-6^{ii}), 125.4 (C-4^{ii}), 122.5 (C-2^{iv}), 118.1 (CN), 116.3 (C-2^{ii}), 111.0 (C-3^{iv}), 82.1 ($C(CH_3)_3$), 81.1 ($C(CH_3)_3$), 79.8 ($C(CH_3)_3$), 52.7 (C-2), 42.7 (C-4), 36.2 (C-1^{i}), 34.4 (C-3), 32.0 (C-1^{i}), 31.2 (C-2^{i}), 28.4 ($C(CH_3)_3$), 28.1 (2x$C(CH_3)_3$); IR (ATR): 2978, 2932, 2232, 1714, 1367, 1148 cm^{-1}; HRMS (HR-ESI) calcd. for [$C_{36}H_{46}N_4O_6$+Na]: 653.3310; found: 653.3296. COSY and ^{1}H/^{13}C correlation were recorded.

(1*S*,3*R*,*E*)-1,3-dicarboxy-6-((*Z*)-8-cyano-11,12-dihydrodibenzo[*c*,*g*][1,2] diazocin-3-yl)hex-5-en-1-aminium chloride, Glu_brAzo1

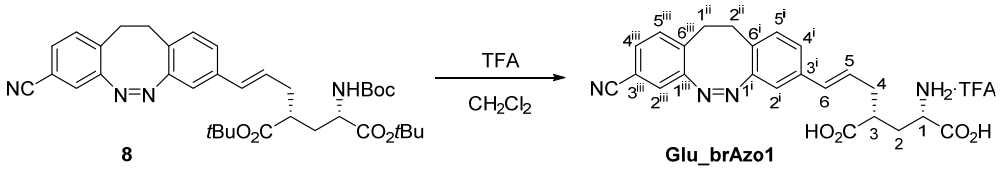

8 **Glu_brAzo1**

To a solution of **8** (45 mg, 0.07 mmol) in CH_2Cl_2 (11 mL), trifluoroacetic acid (4 mL, 52.2 mmol) was added. After stirring 2 h at rt, the solution was concentrated under vacuum. The resulting solid was washed with Et_2O, hexane and EtOAc to furnish **Glu_brAzo1** (30 mg, 0.06 mol, 81% yield) as a brown solid: mp 134-139 ºC (from EtOAc); $[\alpha]_D^{20}$ 20.8 (*c* 0.18, DMSO-d_6); ^{1}H NMR (360 MHz, DMSO-d_6) δ 7.55 (d, $J_{4^{iii},5^{iv}}$ = 7.8 Hz, 1H, H-4^{iii}), 7.44 (s, 1H, H-2^{iii}), 7.34 (d, $J_{5^{iii},4^{iii}}$ = 7.8 Hz, 1H, H-5^{iii}), 7.12 (d, $J_{4^{i},5^{i}}$ =

7.9 Hz, 1H, H-4^{i}), 7.04 (d, $J_{5i,4i}$ = 7.9 Hz, 1H, H-5^{i}), 6.88 (s, 1H, H-2^{i}), 6.37 (d, $J_{6,5}$ = 15.6 Hz, 1H, H-6), 6.15 (m, 1H, H-5), 3.80 (m, 1H, H-1), 2.87 (m, 4H, H-1^{ii}, H-2^{ii}), 2.71 (m, 1H, H-3), 2.50 (m, 2H, H-4), 2.13 (m, 1H, H-2), 1.77 (m, 1H, H-2); ^{13}C NMR (90.5 MHz, DMSO-d_6) δ 175.0/170.9 (2xCOOH), 155.1 (C-1^{iii}), 155.0 (C-1^{i}), 135.9 (C-3^{i}), 134.6 (C-6^{iii}), 131.2 (C-5^{iii}), 131.0 (C-4^{iii}), 130.8 (C-6), 130.4 (C-5^{i}), 127.7 (C-5), 126.3 (C-6^{i}), 125.0 (C-4^{i}), 122.2 (C-2^{iii}), 118.1 (CN), 115.8 (C-2^{i}), 109.6 (C-3^{iii}), 50.9 (C-1), 40.4 (C-3), 35.0 (C-4), 31.3 (C-2), 30.9 (C-1^{ii}), 30.3 (C-2^{ii}); IR (ATR) 2934, 2231, 1675, 1606, 1243, 1200, 1134 cm^{-1}; HRMS (HR-ESI) calcd. for $[C_{23}H_{23}N_4O_4]^+$: 419.1714; found: 419.1718. COSY and ^{1}H/^{13}C correlation were recorded.

(*Z*)-8-bromo-11,12-dihydrodibenzo[*c*,*g*][1,2]diazocine-3-carboxylic acid, 7a

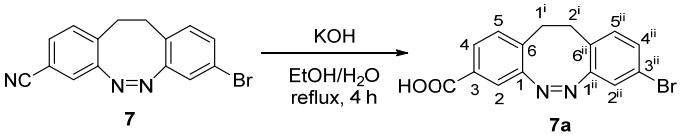

To a solution of nitrile **7** (260 mg, 0.84 mmol) in EtOH (36 mL), a solution of KOH (5.20 g, 92.7 mmol) in H_2O (11 mL) was added dropwise. The mixture was heated at reflux temperature for 4 h. Then, the EtOH was removed under vacuum and the resulting aqueous solution was acidified to pH 4. The product was extracted with EtOAc (3 x 50 mL) and the combined organic extracts were dried over anhydrous Na_2SO_4 and concentrated under vacuum to give **7a** (265 mg, 0.80 mmol, 95% yield) as a black solid: mp > 230 ºC (from EtOAc); ^{1}H NMR (400 MHz, acetone-d_6) δ 7.72 (dd, $J_{4,5}$ = 7.9 Hz, $J_{4,2}$ = 1.7 Hz, 1H, H-4), 7.48 (d, $J_{2,4}$ = 1.7 Hz, 1H, H-2), 7.24 (d, $J_{5,4}$ = 7.9 Hz, 1H, H-5), 7.22 (dd, $J_{4ii,5ii}$ = 8.2 Hz, $J_{4ii,2ii}$ = 2.0 Hz, 1H, H-4^{ii}), 7.11 (d, $J_{2ii,4ii}$ = 2.0 Hz, 1H, H-2^{ii}), 7.06 (d, $J_{5ii,4ii}$ = 8.2 Hz, 1H, H-5^{ii}), 2.94 (m, 4H, H-1^{i}, H-2^{i}); ^{13}C NMR (100.6 MHz, acetone-d_6) δ 166.5 (-COOH), 157.5 (C-1^{ii}), 156.2 (C-1), 134.4 (C-6), 132.7 (C-5^{ii}), 131.3 (C-4^{ii}), 130.9 (C-5), 130.3 (C-3), 129.2 (C-4), 128.4 (C-6^{ii}), 122.1 (C-2^{ii}), 120.5 (C-2), 120.5 (C-3^{ii}), 31.9 (C-1^{i}), 31.3 (C-2^{i}); IR (ATR) 2922, 2852, 2538, 1683, 1430, 1296, 1226 cm^{-1}; HRMS (HR-ESI) calcd. for $[C_{15}H_{10}BrN_2O_2+H]^+$: 331.0077; found: 331.0082. COSY and ^{1}H/^{13}C correlation were recorded.

***tert*-butyl (*Z*)-4-(8-bromo-11,12-dihydrodibenzo[*c*,*g*][1,2]diazocine-3-carboxamido) benzoate, 9**

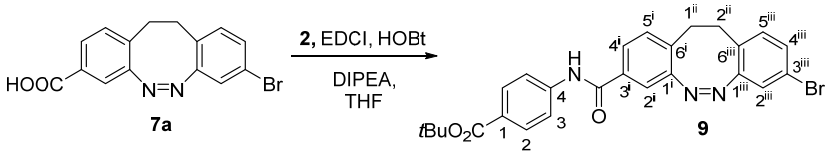

To a solution of acid **7a** (50 mg, 0.15 mmol) in dry THF (7 mL), a solution of amine **2** (35 mg, 0.18 mmol), EDCI·HCl (40 mg, 0.21 mmol), HOBt (32 mg, 0.24 mmol) and DIPEA (0.11 mL, 0.63 mmol) in dry THF (3.6 mL) were added. The reaction mixture was stirred at rt overnight. Then, H_2O (20 mL) was added and the resulting mixture was extracted with CH_2Cl_2 (3 x 20 mL). The combined organic extracts were dried over anhydrous Na_2SO_4, filtered and concentrated under vacuum. The resulting residue was purified by column chromatography (hexane/EtOAc, 3:1) to furnish **9** (60 mg, 0.12 mmol, 78% yield) as a pale yellow solid: mp 226-230 ºC (from EtOAc); ^{1}H NMR (400 MHz, $CDCl_3$) δ 7.98 (d, $J_{2,3}$ = 8.7 Hz, 2H, H-2), 7.90 (br s, 1H, CONH), 7.67 (d, $J_{3,2}$ = 8.7 Hz, 2H, H-3), 7.57 (dd, $J_{4^i,5^i}$ = 8.0 Hz, $J_{4^i,2^i}$ = 1.9 Hz, 1H, H-4^i), 7.37 (d, $J_{2^i,4^i}$ = 1.9 Hz, 1H, H-2^i), 7.16 (dd, $J_{4^{iii},5^{iii}}$ = 8.2 Hz, $J_{4^{ii},2^{ii}}$ = 2.0 Hz, 1H, H-4^{iii}), 7.13 (d, $J_{5^i,4^i}$ = 8.0 Hz, 1H, H-5^i), 7.01 (d, $J_{2^{iii},4^{iii}}$ = 2.0 Hz, 1H, H-2^{iii}), 6.88 (d, $J_{5^{ii},4^{ii}}$ = 8.2 Hz, 1H, H-5^{iii}), 2.90 (m, 4H, H-1^{ii}, H-2^{ii}), 1.59 (s, 9H, C(CH_3)$_3$); ^{13}C NMR (100.6 MHz, $CDCl_3$) δ 165.3 (C, ester), 164.5 (C, amide), 156.1 (C-1^{iii}), 155.4 (C-1^i), 141.5 (C-4), 133.6 (C-3^i), 132.5 (C-6^i), 131.4 (C-5^{iii}), 130.8 (C-2, C-4^{iii}), 130.6 (C-5^i), 128.2 (C-1), 126.8 (C-6^{iii}), 126.2 (C-4^i), 122.0 (C-2^{iii}), 120.6 (C-3^{iii}), 119.3 (C-3), 118.0 (C-2^i), 81.1 (*C*(CH_3)$_3$), 31.7 (C-1^{ii}), 31.1 (C-2^{ii}), 28.4 (C(*C*H_3)$_3$); IR (ATR) 3415, 2965, 1705, 1673, 1521, 1290, 1161, 1103 cm^{-1}; HRMS (HR-ESI) calcd. for [$C_{26}H_{24}BrN_3O_3$+H]$^+$: 506.1074; found: 506.1085. COSY and ^{1}H/^{13}C correlation were recorded.

di-tert-butyl (2*S*,4*R*)-2-((*tert*-butoxycarbonyl)amino)-4-((*E*)-3-((*Z*)-8-((4-(*tert*-butoxy carbonyl)phenyl)carbamoyl)-11,12-dihydrodibenzo[c,g][1,2]diazocin-3-yl)allyl)pentanedioate, 9a

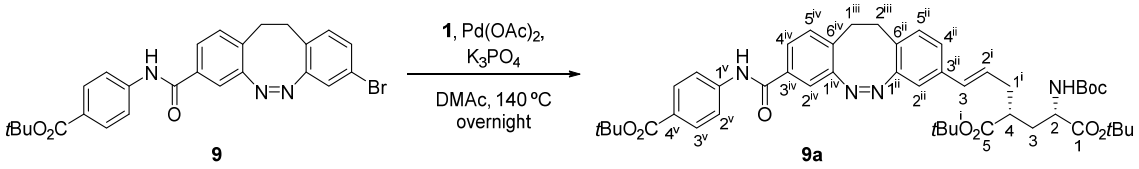

A mixture of diazocine **9** (60 mg, 0.12 mmol), glutamate derivative **1** (57 mg, 0.14 mmol), $Pd(OAc)_2$ (3 mg, 13 μmol) and K_3PO_4 (35 mg, 0.16 mmol) in DMAc (1.0 mL) under argon atmosphere was heated at 140 ºC overnight. Then, the solvent was evaporated and the resulting residue was purified by column chromatography (hexane/EtOAc, 5:1) to give **9a** (50 mg, 60 μmol, 51% yield) as a yellow foam: ^{1}H NMR (360 MHz, $CDCl_3$) δ 8.10 (s, 1 H, -NHCO), 7.95 (d, $J_{3^v,2^v}$ = 8.2 Hz, 2H, H-3^v), 7.66 (d, $J_{2^v,3^v}$ = 8.2 Hz, 2H, H-2^v), 7.55 (d, $J_{4^{iv},5^{iv}}$ = 8.0 Hz, 1H, H-4^{iv}), 7.36 (s, 1H, H-2^{iv}), 7.11 (d, $J_{5^{iv},4^{iv}}$ = 8.0 Hz, 1H, H-5^{iv}), 6.98 (d, $J_{4^{ii},5^{ii}}$ = 8.0 Hz, 1H, H-4^{ii}), 6.90 (d, $J_{5^{ii},4^{ii}}$ = 8.0 Hz, 1H, H-5^{ii}), 6.79 (s, 1H, H-2^{ii}), 6.26 (d, $J_{3^i,2^i}$ = 15.7 Hz, 1H, H-3^i), 6.02 (m, 1H, H-2^i), 4.99 (d,

$J_{NHBoc,2}$ = 8.5 Hz, 1H, NHBoc), 4.21 (m, 1H, H-2), 2.97 (m, 2H, H-1^{iii}, H-2^{iii}), 2.79 (m, 2H, H-1^{iii}, H-2^{iii}), 2.43 (m, 2H, H-1^{i}, H-4), 2.31 (m, 1H, H-1^{i}), 2.13 (m, 1H, H-3), 1.68 (m, 1H, H-3), 1.58 (s, 9H, C(CH$_3$)$_3$), 1.40 (s, 18H, C(CH$_3$)$_3$), 1.37 (s, 9H, C(CH$_3$)$_3$); ^{13}C NMR (90.6 MHz, CDCl$_3$) δ 173.9 (C-5), 171.7 (C-1), 165.4 (C, ester), 164.7 (C, amide), 155.4 (C, carbamate, C-1^{ii}, C-1^{iv}), 141.7 (C-1^{v}), 133.5 (C-3^{ii}), 133.3 (C-3^{iv}), 132.9 (C-6^{iv}), 131.1 (C-3^{i}), 130.7 (C-3^{v}), 130.5 (C-5^{iv}), 130.1 (C-5^{ii}), 127.9 (C-2^{i}, C-4^{v}), 126.4 (C-6^{ii}), 126.0 (C-4^{iv}), 125.3 (C-4^{ii}), 119.2 (C-2^{v}), 118.0 (C-2^{iv}), 116.5 (C-2^{ii}), 82.1 (*C*(CH$_3$)), (81.0 (*C*(CH$_3$)$_3$), 79.8 (*C*(CH$_3$)$_3$), 52.7 (C-2), 42.7 (C-4), 36.2 (C-1^{i}), 34.4 (C-3), 31.8 (C-1^{i}), 31.4 (C-2^{i}), 28.4 (C(*C*H$_3$)$_3$), 28.3 (C(*C*H$_3$)$_3$), 28.1 (2xC(*C*H$_3$)$_3$); IR (ATR) 3343, 2983, 2931, 1710, 1528, 1148 cm^{-1}; HRMS (HR-ESI) calcd. for [C$_{47}$H$_{60}$N$_4$O$_9$+H]: 825.4433; found: 825.4418. COSY and ^{1}H/^{13}C correlation were recorded.

(1*S*,3*R*,*E*)-1,3-dicarboxy-6-((*Z*)-8-((4-carboxyphenyl)carbamoyl)-11,12-dihydro dibenzo[c,g][1,2]diazocin-3-yl)hex-5-en-1-aminium trifluoroacetate, Glu_brAzo2

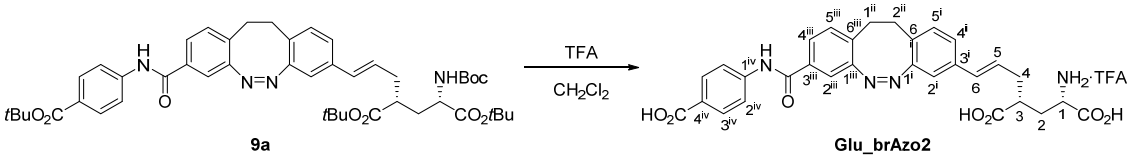

9a **Glu_brAzo2**

To a solution of **9a** (50 mg, 61 µmol) in CH_2Cl_2 (9 mL), trifluoroacetic acid (4.5 mL, 59 mmol) was added. The mixture was stirred for 2 h and the solvent was evaporated under vacuum. The resulting solid was washed with Et_2O, hexane and EtOAc to give **Glu_brAzo2** (33 mg, 0.049 mmol, 82% yield) as a pale orange solid: mp > 230 ºC (from EtOAc); $[\alpha]_D^{20}$ -6.0 (*c* 0.25, DMSO-d$_6$); ^{1}H NMR (400 MHz, DMSO-d$_6$) δ 10.50 (s, 1 H, -NHCO), 7.92 (d, $J_{3iv,2iv}$ = 8.7 Hz, 2H, H-3^{iv}), 7.85 (d, $J_{2iv,3iv}$ = 8.7 Hz, 2H, H-2^{iv}), 7.68 (d, $J_{4iii,5iii}$ = 7.9 Hz, 1H, H-4^{iii}), 7.46 (s, 1H, H-2^{iii}), 7.29 (d, $J_{5iii,4iii}$ = 7.9 Hz, 1H, H-5^{iii}), 7.11 (d, $J_{4i,5i}$ = 8.0 Hz, 1H, H-4^{i}), 7.06 (d, $J_{5i,4i}$ = 8.0 Hz, 1H, H-5^{i}), 6.90 (s, 1H, H-2^{i}), 6.34 (d, $J_{6,5}$ = 15.5 Hz, 1H, H-6), 6.15 (m, 1H, H-5), 3.29 (m, 1H, H-1), 2.86 (m, 4H, H-1^{ii}, H-2^{ii}), 2.68 (m, 1H, H-3), 2.50 (m, 2H, H-4), 2.04 (m, 1H, H-2), 1.65 (m, 1H, H-2); ^{13}C NMR (90.6 MHz, DMSO-d$_6$) δ 172.8/171.8 (2xCOOH), 166.9(COOH), 164.7 (C, amide), 155.1 (C-1^{iii}), 154.6 (C-1^{i}), 143.0 (C-1^{iv}), 135.9 (C-3^{i}), 133.0 (C-3^{iii}), 132.3 (C-6^{iii}), 130.2 (C-5^{i}, C-5^{iii}, C-3^{iv}), 128.2 (C-6), 126.6 (C-5, C-6^{i}), 125.6 (C-4^{iii}, C-4^{iv}), 124.7 (C-4^{i}), 119.5 C-2^{iv}), 118.0 (C-2^{iii}), 116.0 (C-2^{i}), 50.7 (C-1), 40.1 (C-3), 35.5 (C-4), 31.1 (C-2), 30.9 (C-1^{ii}), 30.5 (C-2^{ii}); IR (ATR) 2923, 1676, 1599, 1521, 1247, 1176 cm^{-1}; HRMS (HR-ESI) calcd. for [C$_{30}$H$_{29}$N$_4$O$_7$]: 557.2031; found: 557.2040. COSY and ^{1}H/^{13}C correlation were recorded.

Computational, photochemical and biological supplementary methods

Molecular docking calculations: Docking calculations were performed with GOLD5.6.3[3] program on the rigid crystallographic structure of GluK2 Ligand Binding Domain retrieved from the Protein Data Bank (PDB code: 4H8I).[4] H++ web-server[5] was used to add missing hydrogen atoms to the protein pdb file and to determine the protonation states of ionizable residues at pH = 7.0. All co-crystallized ligands, and water molecules were removed. The structures of *trans*-**Glu_brAzo1** and *cis*-**Glu_brAzo1** were built with standard bond lengths and angles using Gaussview[6] and UCSF Chimera[7] codes. Those structures were further minimized using Quantum Mechanics at the B3LYP/6-31G(d) level with the Gaussian09 package.[8] The *trans*-**Glu_brAzo2** and *cis*-**Glu_brAzo2** initial structures were built from the coordinates of *trans*-**Glu_brAzo1** and *cis*-**Glu_brAzo1** QM minima, respectively, by replacing the cyano substituent by the bulky -CONH-*p*-C6H4COOH group, and the corresponding QM minima were also located. The four minimized compounds and the protein were further prepared for docking by assigning GOLD atom types to all the atoms by means of Hermes (GOLD 3D Visualizer).

To ensure a complete exploration of the conformational space of the four ligands in the binding site of the protein, the maximum efficiency of the genetic algorithm was selected in the docking setup. All the parameters of the genetic algorithm were set to the default values of the program and partial flexibility was assigned to the ligands. The binding site of the receptor was defined as all atoms within 15 Å of a conveniently specified central point (given by its X, Y, Z coordinates). 100 binding solutions for each ligand were generated. The Chemscore fitness function[9] was selected to estimate the binding affinities of the four ligands. The obtained poses were ranked based on those affinity docking scores (kJ/mol) and the best solution for each ligand was selected.

Photochemical characterization of Glu_brAzo1 and Glu_brAzo2: All spectroscopic and photochemical experiments were carried out in HPLC- or spectroscopy-quality solvents. Steady-state UV-vis absorption measurements were recorded on a HP 8453 spectrophotometer with temperature control. The UV-vis absorption spectra of *trans*-**Glu_brAzo1** and *trans*-**Glu_brAzo2** in PBS:DMSO 1:1 was estimated from the absorption spectra of as-synthesized *cis*-**Glu_brAzo1** and *cis*-**Glu_brAzo2** and of a well-known mixture of their *cis* and *trans* isomers, the composition of which was measured by ^{1}H NMR in DMSO-d_6. Isomerization quantum yields were determined relative to 1,2-bis(5-chloro-2-methyl-3-thienyl)perfluorocyclopentene in hexane ($\Phi_{ring\ opening}$ = 0.13[10]). Different excitation sources were used in the photochemical

experiments depending on the spectral requirements: a cw DPSS laser (λ_{exc} = 405 nm, SciTec) for *cis-trans* photoisomerization, and the second harmonic of a ns-pulsed Nd:YAG laser (λ_{exc} = 532 nm, Brilliant, Quantel) for *trans-cis* photoisomerization.

Cell line and transfection: HEK293 tsA201 cell line (SV40-transformed, Human Embryonic Kidney 293 cells) was maintained at 37 ºC in a 5% CO_2 humid incubator with Dulbecco's Modified Eagle Medium/Nutrient Mixture F-12 media (DMEM) (1:1, Invitrogen) supplemented with 10% Fetal Bovine Serum (FBS) and 1% Penicillin/Streptomycin. Cells transiently expressed the receptor subunit GluK2 or GluK1(Q)-2b(GGAA). The expression plasmid for GluK2 was kindly provided by Ehud Y. Isacoff (University of California). GluK2 was subcloned into EcoRI site of the pCDNA3.1 expression vector. To obtain the GluK2-eGFP pCDNA3 construct, a fragment spanning the C-terminal domain of GluK2 and eGFP was amplified by PCR using AfeI/XbaI flanked primers and subcloned into GluK2-pCDNA3 plasmid by replacing the former AfeI/XbaI cassette. GluK1(Q)-2b(GGAA) was kindly provided by G. Swanson (Northwestern University, Feinberg School of Medicine), with the endoplasmic reticulum retention motif of the carboxy-terminal mutated to increase surface expression.[11] DNA–X-tremGENE 9 Transfection Reagent (Roche) mix was used following manufacturer's instructions with a Reagent:DNA ratio of 3:1. GluK1(Q)-2b-GGAA plasmid was co-transfected with peGFP with a Transfection Reagent:GluK1:eGPF ratio of 3:1:0.1.

The mix was incubated for 20 min at room temperature, meanwhile cells were detached and freshly plated into a 12-mulltiwell plate at a density of 3 × 105 cells before the DNA-Transfection Reagent mix was added dropwise into each well. Experiments were performed after 48–72 h, and the day before the experiment cells were plated at low density on 16-mm coverslips (Fisher Scientific) treated with collagen(Sigma-Aldrich) to allow cell adhesion.

Electrophysiology: Whole-cell voltage-clamp recordings were done using an EPC-10 amplifier and data at 10 kHz was acquired with amplifier's software Patch Master (HEKA). Bath solution was composed of (in mM): 140 NaCl, 1 $MgCl_2$, 2.5 KCl, 10 HEPES, 2.5 $CaCl_2$ and 10–20 glucose to fix osmolarity to 310 mOsm·kg^{-1}, while pH 7.42 was adjusted with NaOH. Borosilicate glass pipettes were pulled with a typical resistance of 4–6 MΩ for HEK293 cells. Pipette solution contained (in mM): 120 cesium methanosulfonate, 10 TEA-Cl, 5 $MgCl_2$, 3 Na_2ATP, 1 Na_2GTP, 20 HEPES, 0.5 EGTA; osmolarity was 290 mOsm·kg^{-1} and pH 7.2 was adjusted with CsOH.

Before starting the recording, cells were incubated 10 min with 0.3 mg mL^{-1} Concanavalin A (Sigma) —to block GluK1 and GluK2 desensitization— on an ES based on $NMDG^+$ (to avoid depolarization due to open GluRs, in mM): 110 $NMDG^+$, 2.5 KCl, 1 $MgCl_2$, 10 HEPES, 10–20 glucose to fix osmolarity to 300 $mOsm \cdot kg^{-1}$, while pH 7.4 was adjusted with HCl. Before placing the coverslip to the recording chamber, cells were washed again with bath solution.

Light stimulation was done by illumination of the entire focused field using a Polychrome V monochromator (TILL Photonics) connected through the back port of an IX71 inverted microscope (Olympus) with a XLUMPLFLN 20XW x20/1 water immersion objective (Olympus). For automatically controlling wavelength, the monochromator was connected to the EPC-10 amplifier via Photochromic Manual Control (TILL Photonics) and controlled with the photometry module of Patch Master. Light power density measured with a Newport 1916-C light meter after the objective was 22.0 $\mu W\ mm^{-2}$ for 380 nm, 45.9 $\mu W\ mm^{-2}$ for 460 nm and 47.4 $\mu W\ mm^{-2}$ for 500 nm.

One-photon action spectrum characterization was done during voltage-clamp recordings applying a train of 1 s light-pulses at different wavelengths (for the whole action spectrum, we ranged wavelengths from 300 to 600 nm, with 10 nm steps) with 5 s delay between pulses in which light was switched to 530 nm to *trans-cis* back-isomerize for activation spectrum, and to 390nm for deactivation spectrum.

Rat hippocampal neural primary culture. All procedures were conducted in accordance with the European guidelines for animal care and use in research, and were approved by the Animal Experimentation Ethics Committee at the University of Barcelona (Spain). Low-density primary hippocampal cultures were prepared from newborn P0-P3 pups from Sprague Dawley rat and maintained in cell culture for 1-2 weeks in coverslips coated with poly-L-lysine (Sigma-Aldrich), as previously described.[12-14].

Cells were cultured with complete medium (Neurobasal A, B-27 5%, GlutaMax (0.5x), glucose 15mM, penicillin (5 U ml−1) and streptomycin (5 µg ml−1)). Within 48-72 h an anti-mitotic treatment with AraC 5 µM is done to avoid fibroblast and astrocyte proliferation. Half of the medium in each well was changed every 3-4 days.

***Electrophysiology recording conditions for rat hippocampal neurons*:** Voltage and current-clamp recordings under whole-cell configuration were done using an EPC-10 amplifier and data at 10 kHz was acquired with amplifier's software Patch Master

(HEKA). Bath solution was composed of (in mM): 140 NaCl, 2 MgCl, 2.5 KCl, 10 HEPES, 0.2 $CaCl_2$ and 10–20 mM glucose to fix osmolarity to 310 mOsm·kg–1, pH 7.42 adjusted with NaOH. Borosilicate glass pipettes were pulled with a typical resistance of 6–8 MΩ for neurons. Pipette solution contained (in mM): 130 KCl, 5 $MgCl_2$, 3 Na_2ATP, 1 Na_2GTP, 20 HEPES, 0.5 EGTA. Osmolarity is adjusted at 289 mOsm·kg–1 and pH 7.2 adjusted with KOH. During recordings, neurons were maintained at room temperature (r.t., 25-27 °C) in a continuous perfusion of bath solution.

Data analysis and statistics: Amplitude of photocurrents were analyzed using IgorPro (Wavemetrics). Displayed whole-cell current traces have been filtered using the infinite impulse response digital filter from IgorPro (low-pass filter with cutoff of 50 Hz). The drift in current observed during light spectra recordings was corrected where appropriate with the IgorPro (WaveMetrics) software using a custom-made macro for drift correction.

Figure S1. Molecular docking simulations

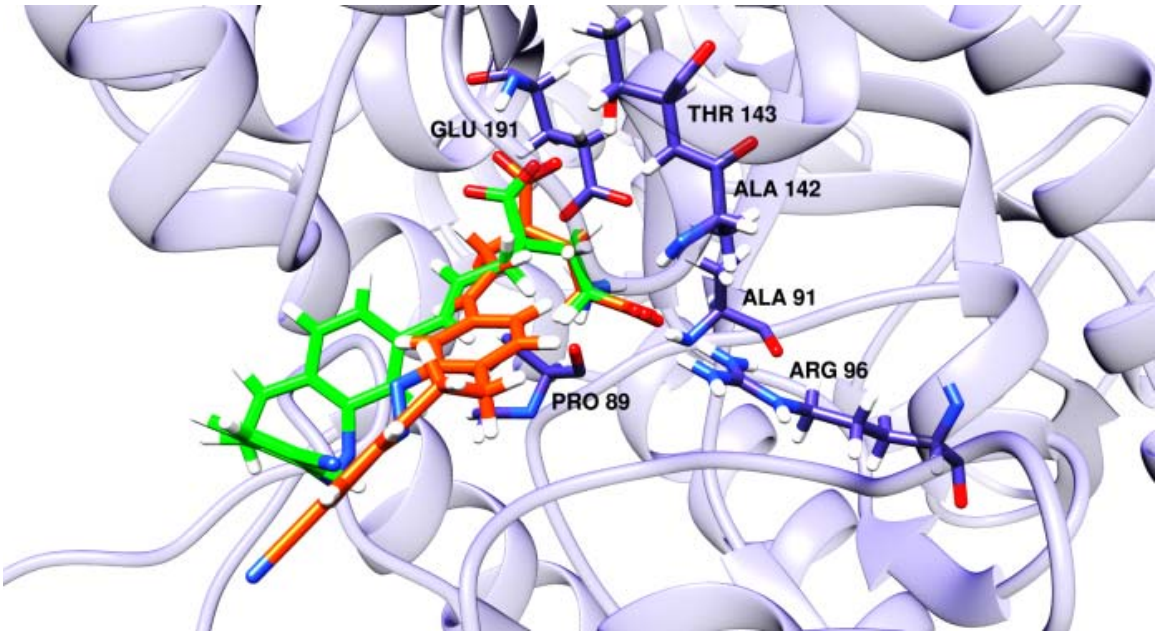

Figure S1. Best docking solutions for *trans*-**Glu_brAzo1** (orange) and *cis*-**Glu_brAzo1** (green) in GluK2. The protein residues interacting with the glutamate groups are also indicated. Oxygen, nitrogen and hydrogen atoms are depicted in red, blue and white, respectively.

Figures S2-S7 and Table S1. Photoisomerization of Glu_brAzo1 and Glu_brAzo2

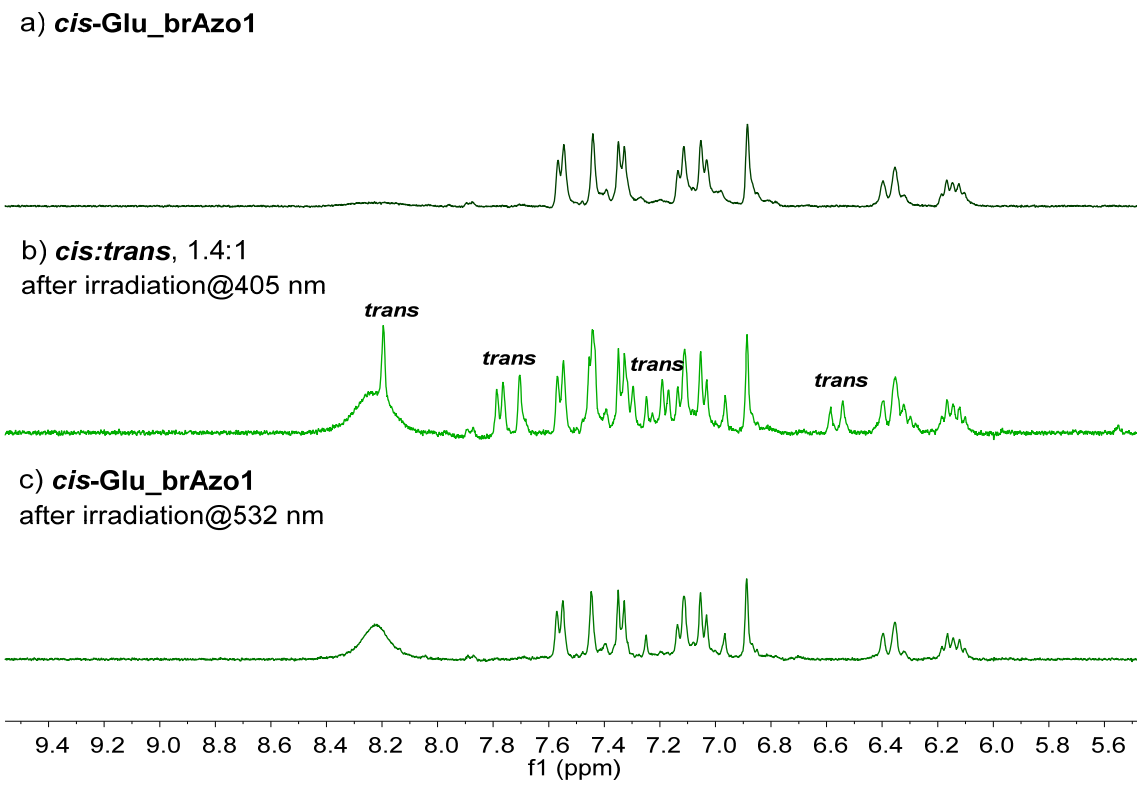

Figure S2. Low-field region of the ^{1}H NMR spectra (360 MHz, DMSO-d_6) of **Glu_brAzo1**: (a) freshly prepared (*cis* isomer); (b) after irradiation at λ_{exc} = 405 nm (power = 280 mW) for 3 h (*cis*:*trans* 1.4:1 mixture); (c) after irradiation of (b) at λ_{exc} = 532 nm (power = 100 mW) for 3 h (*cis* isomer).

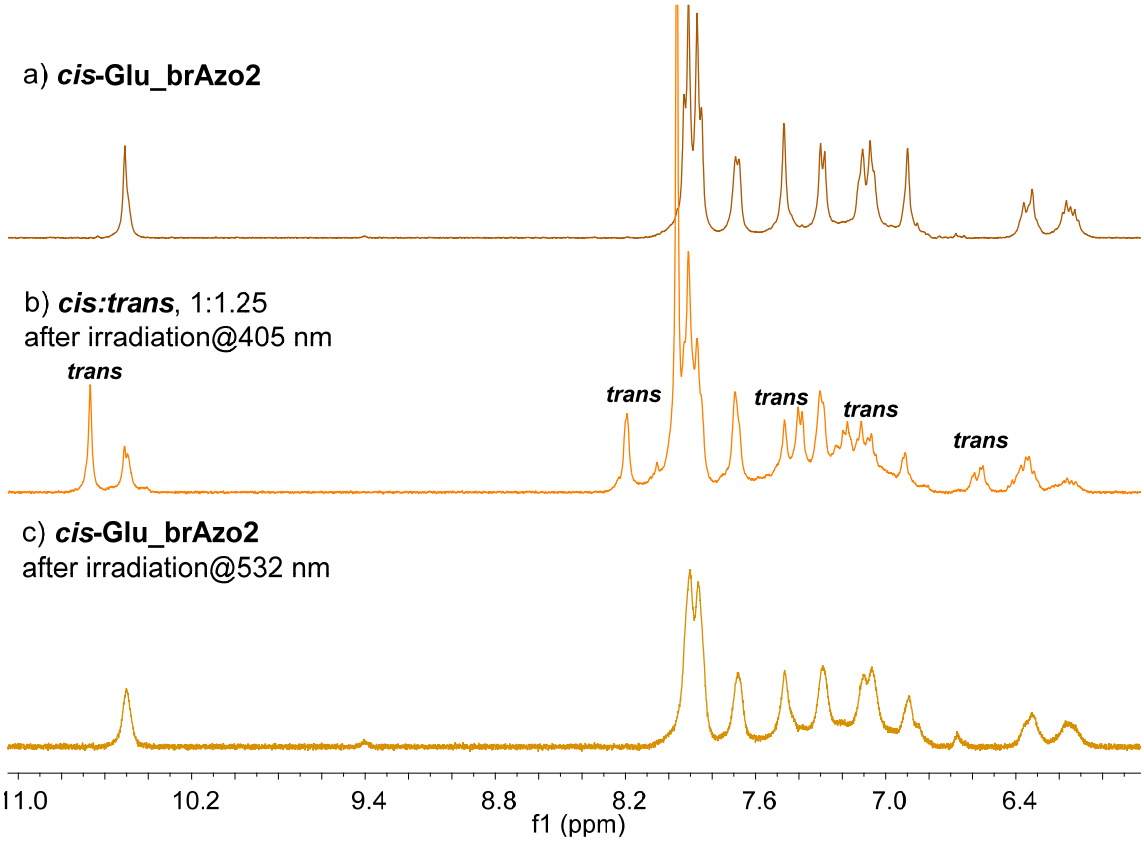

Figure S3. Low-field region of the ^{1}H NMR spectra (400 MHz, DMSO-d_6) of **Glu_brAzo2**: (a) freshly prepared (*cis* isomer); (b) after irradiation at λ_{exc} = 405 nm (power = 280 mW) for 3 h (*cis*:*trans* 1:1.25 mixture); (c) after irradiation of (b) at λ_{exc} = 532 nm (power = 100 mW) for 3 h (*cis* isomer).

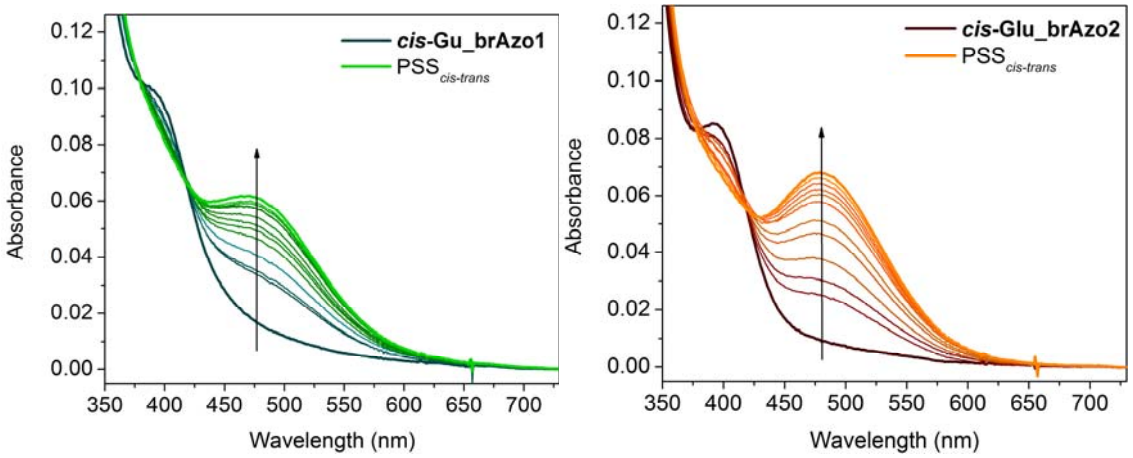

Figure S4. Absorption spectra of **Glu_brAzo1** and **Glu_brAzo2** in PBS:DMSO 1:1 upon irradiation of their *cis* isomer at λ_{exc} = 405 nm (power = 88 mW).

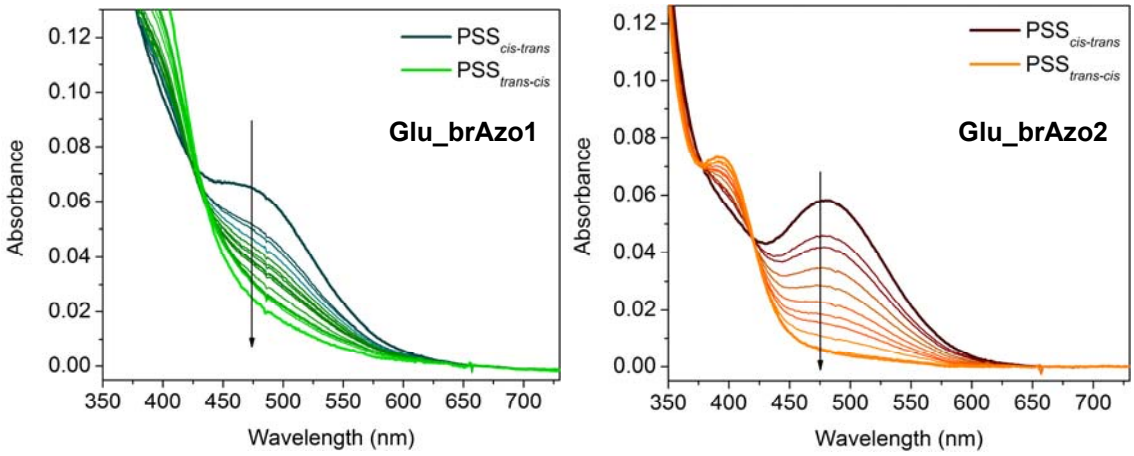

Figure S5. Absorption spectra of **Glu_brAzo1** and **Glu_brAzo2** in PBS:DMSO 1:1 upon irradiation at λ_{exc} = 532 nm (power = 10 mW) of the *cis-trans* photostationary mixture previously prepared at λ_{exc} = 405 nm.

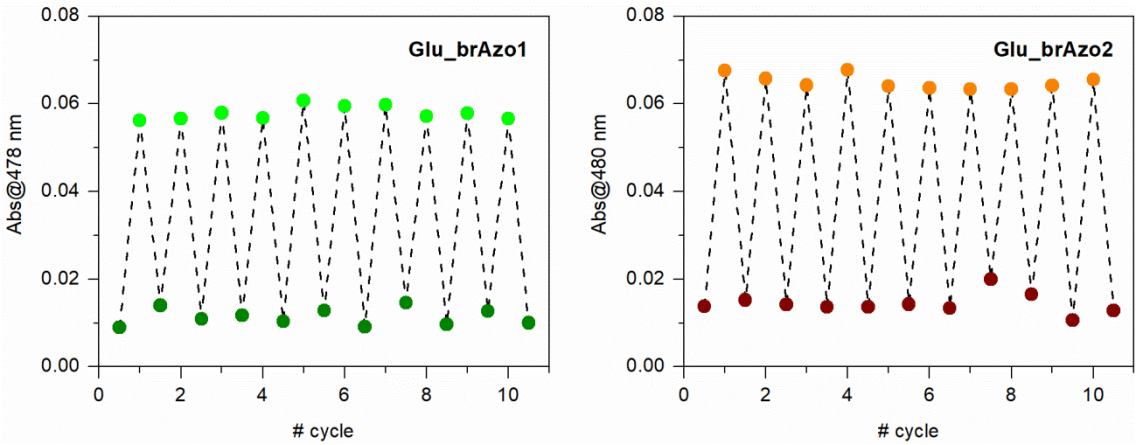

Figure S6. Variation of the absorption at 395 and 478 nm of **Glu_brAzo1** and **Glu_brAzo2** in PBS:DMSO 1:1 upon consecutive cycles of *cis-trans* (λ_{exc} = 405 nm, 280 mW) and *trans-cis* photoisomerization (λ_{exc} = 532 nm, power = 230 mW).

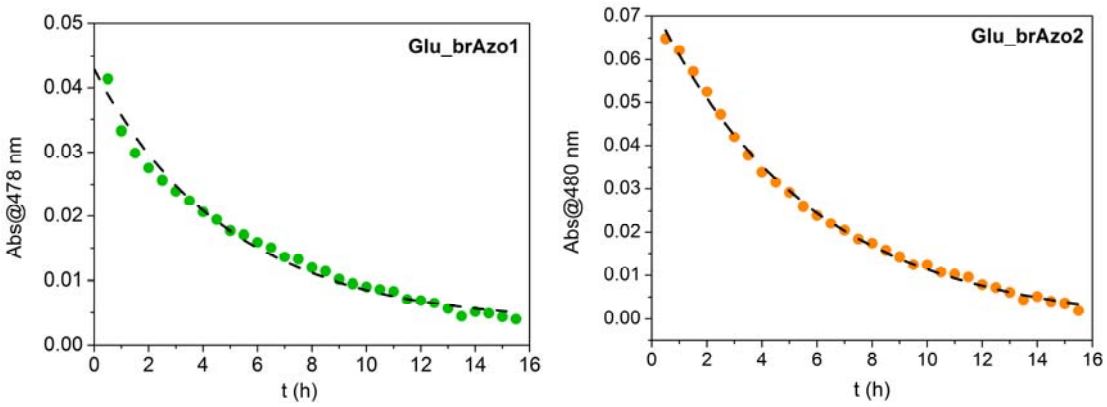

Figure S7. Variation of the absorption at $\lambda_{abs,max}^{trans}$ of the *cis-trans* photostationary state mixture of **Glu_brAzo1** and **Glu_brAzo2** in the dark at 25ºC in PBS:DMSO 1:1. At these conditions, thermal *trans-cis* back-isomerization takes place, thus restoring the initial concentration of the *cis* state of the ligands. Points correspond to the experimental data, while lines were obtained from monoexponential fits.

Table S1. Photochemical properties of **Glu_brAzo1** and **Glu_brAzo2** in PBS:DMSO 1:1.

	$\lambda^{cis}_{abs,max}$ [a] (nm)	$\lambda^{trans}_{abs,max}$ [a] (nm)	$\Phi_{cis\text{-}trans}$	$\Phi_{trans\text{-}cis}$	%*trans* $PSS_{cis\text{-}trans}$	%*cis* $PSS_{trans\text{-}cis}$	τ_{trans} (h)
Glu_brAzo1	392	478	0.11	0.89	47	100	6.8
Glu_brAzo2	395	480	0.13	0.86	60	100	5.6

[a] Data for the n-π* band. [b] $t_{1/2}$ = 4.7 and 3.9 h, respectively.

Figures S8-S11. Photomodulation of GluK1 and GluK2 in HEK293 cells using Glu_brAzo1 and Glu_brAzo2

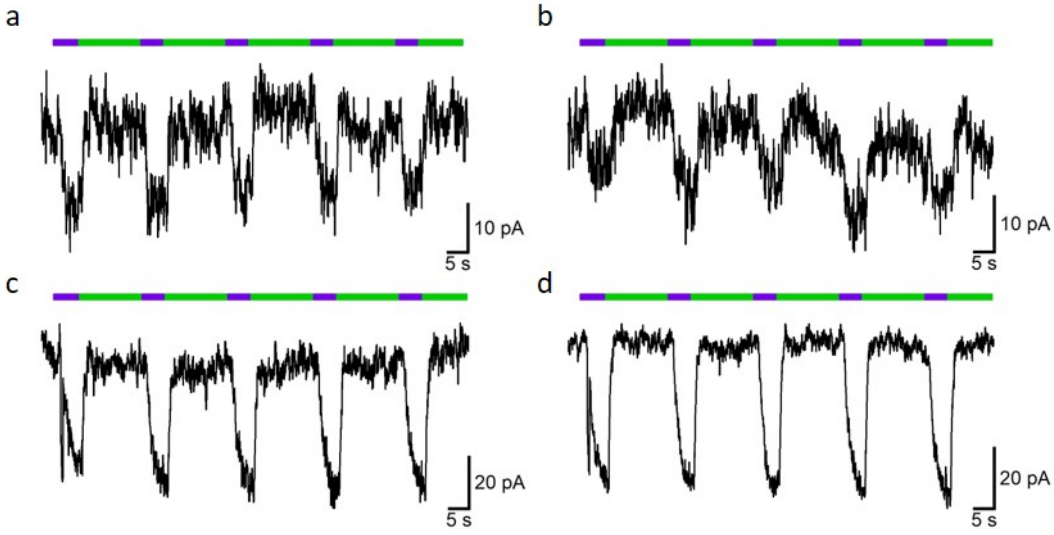

Figure S8. Light-dependent inward currents measured for HEK293 cells expressing GluK1 and GluK2. (a-b) HEK293 cells transfected with GluK1 and perfused with (a) *cis*-**Glu_brAzo1** (100μM), and (b) *cis*-**Glu_brAzo2** (100μM). (c-d) HEK293 cells transfected with GluK2 and perfused with (c) *cis*-**Glu_brAzo1** (100μM), and (d) *cis*-**Glu_brAzo2** (100μM). Light pulses at λ_{exc} = 390 nm (purple bars) were employed to induce *cis-trans* photoisomerization, which in all the cases resulted in larger electrophysiological currents (i.e. receptor activation and channel opening). Irradiation at λ_{exc} = 530 nm (green bars) was used to trigger *trans-cis* back-isomerization and recover the initial signal (i.e. receptor deactivation and channel closing).

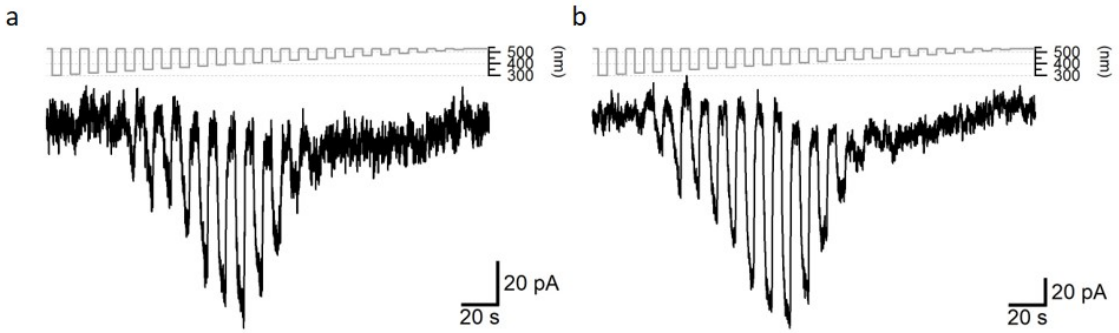

Figure S9. Activation spectra of (a) **Glu_brAzo1** (100μM) and (b) **Glu_brAzo2** (100μM) in HEK293 cells transfected with GluK2. Wavelength excitation to promote *cis-trans* photoisomerization and receptor activation ranges from 300 nm to 530 nm. In all the cases, *trans-cis* back-isomerization was achieved with pulses at λ_{exc} = 530 nm.

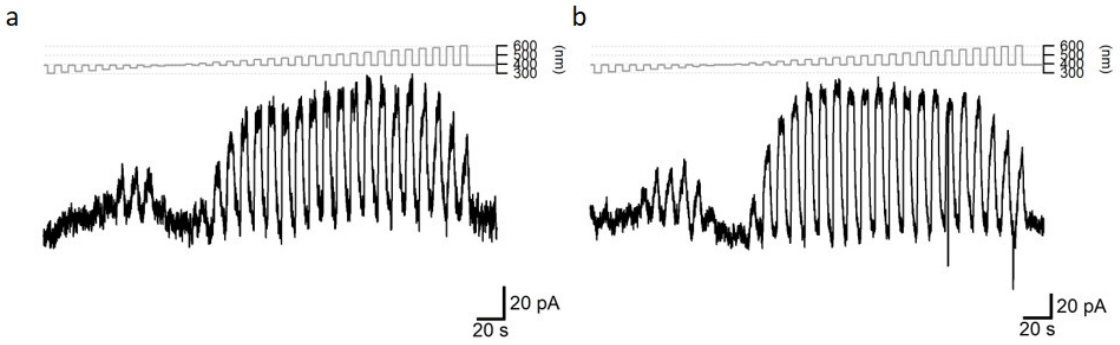

Figure S10. Deactivation spectra of (a) **Glu_brAzo1** (100μM) and (b) **Glu_brAzo2** (100μM) in HEK293 cells transfected with GluK2. Wavelength excitation to promote *trans-cis* photoisomerization and receptor deactivation ranges from 300 nm to 600 nm. In all the cases, *cis-trans* isomerization was previously conducted with pulses at λ_{exc} = 390 nm.

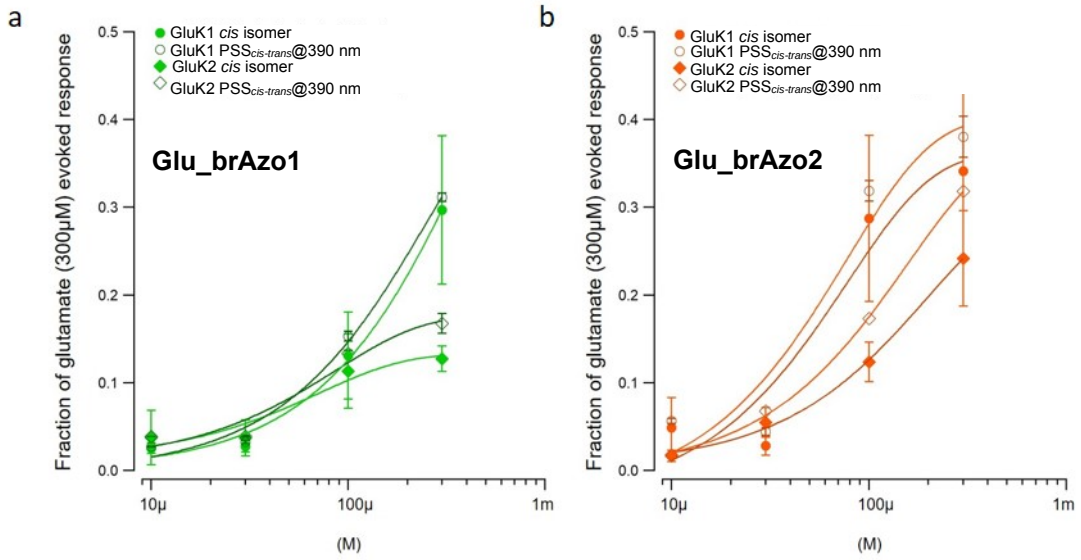

Figure S11. Dose-response curves of (a) **Glu_brAzo1** and (b) **Glu_brAzo2** in HEK293 cells transfected with GluK1 and GluK2. Measurements were conducted from 10 to 300 μM for their *cis* isomer and the *trans-cis* mixture obtained at λ_{exc} = 390 ($PSS_{cis-trans}$@390 nm).

Figures S12. Photoactivation of rat hippocampal neurons using Glu_brAzo1 and Glu_brAzo2

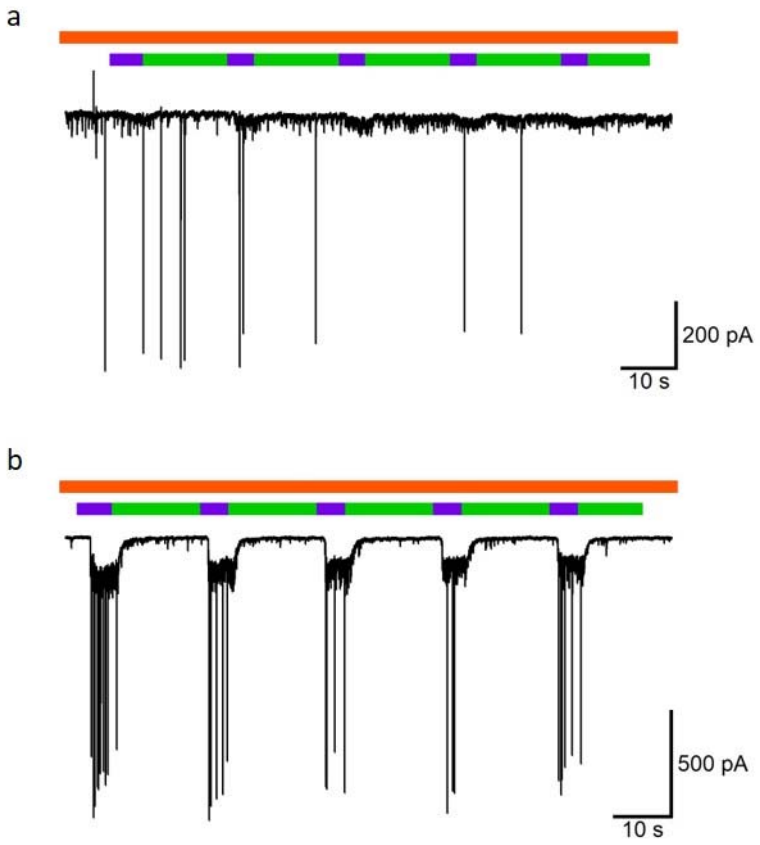

Figure S12. Whole-cell voltage clamp recording of rat hippocampal neurons in culture. Perfusion of 30 μM of (a) **Glu_brAzo1** and (b) **Glu_brAzo2**. Light activation is induced by pulses at λ_{exc} = 390 and 530 nm (purple and green bars, respectively).

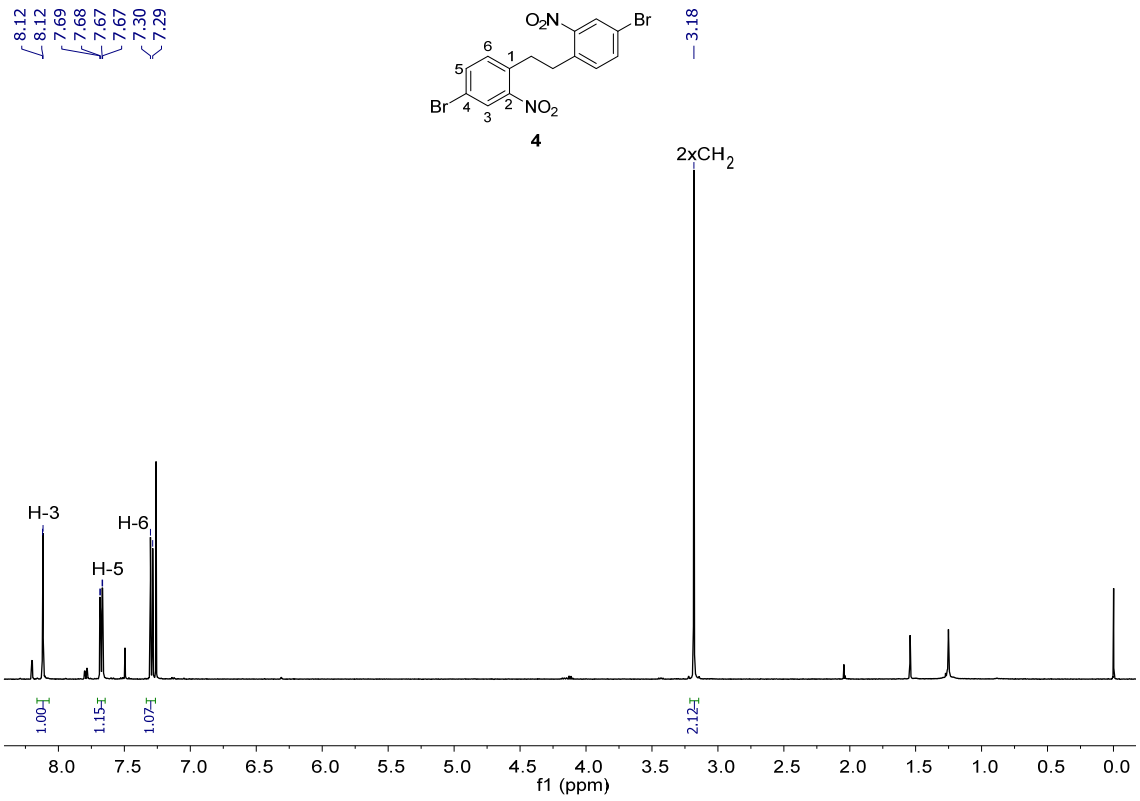

^{1}H NMR (500 MHz, $CDCl_3$)

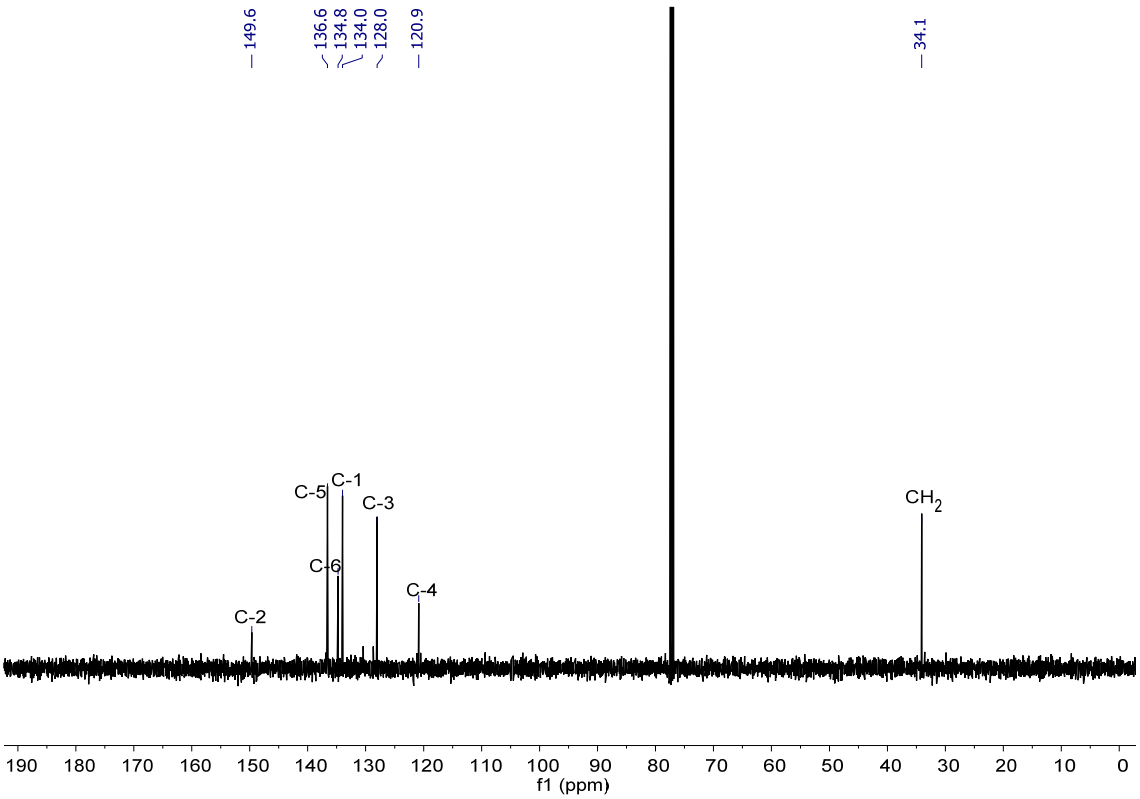

^{13}C NMR (125.8 MHz, $CDCl_3$)

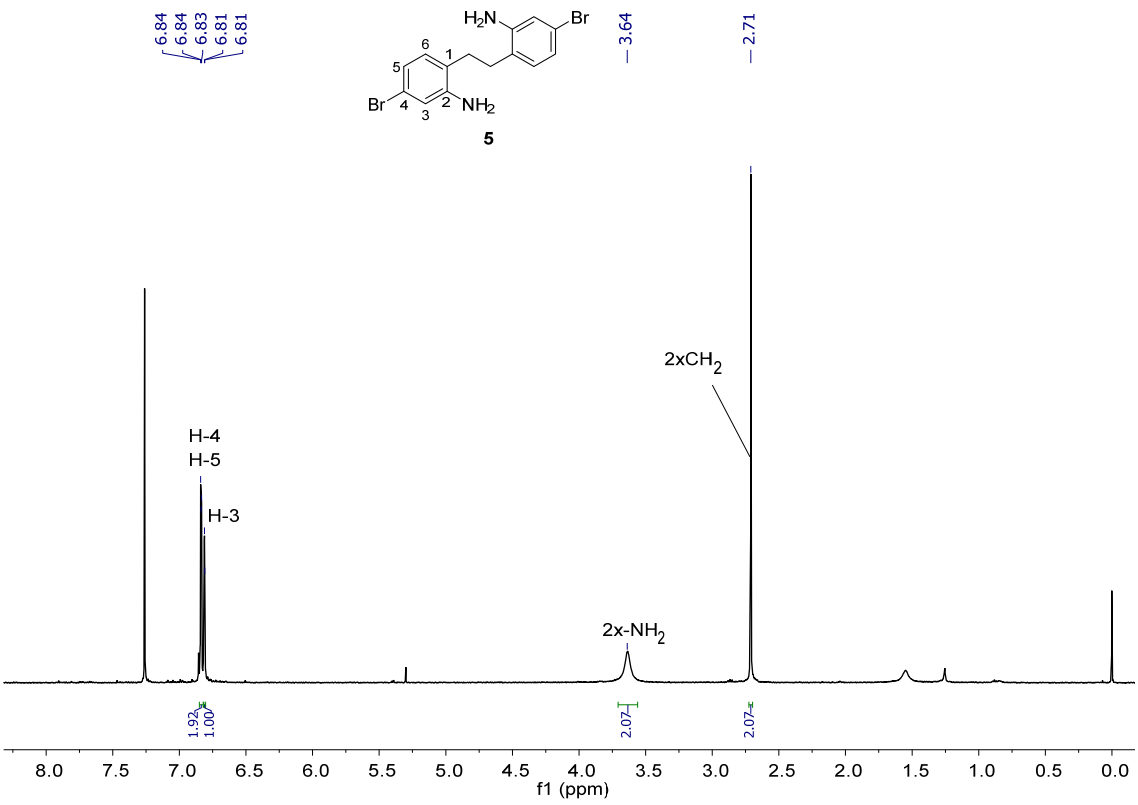

^{1}H NMR (500 MHz, $CDCl_3$)

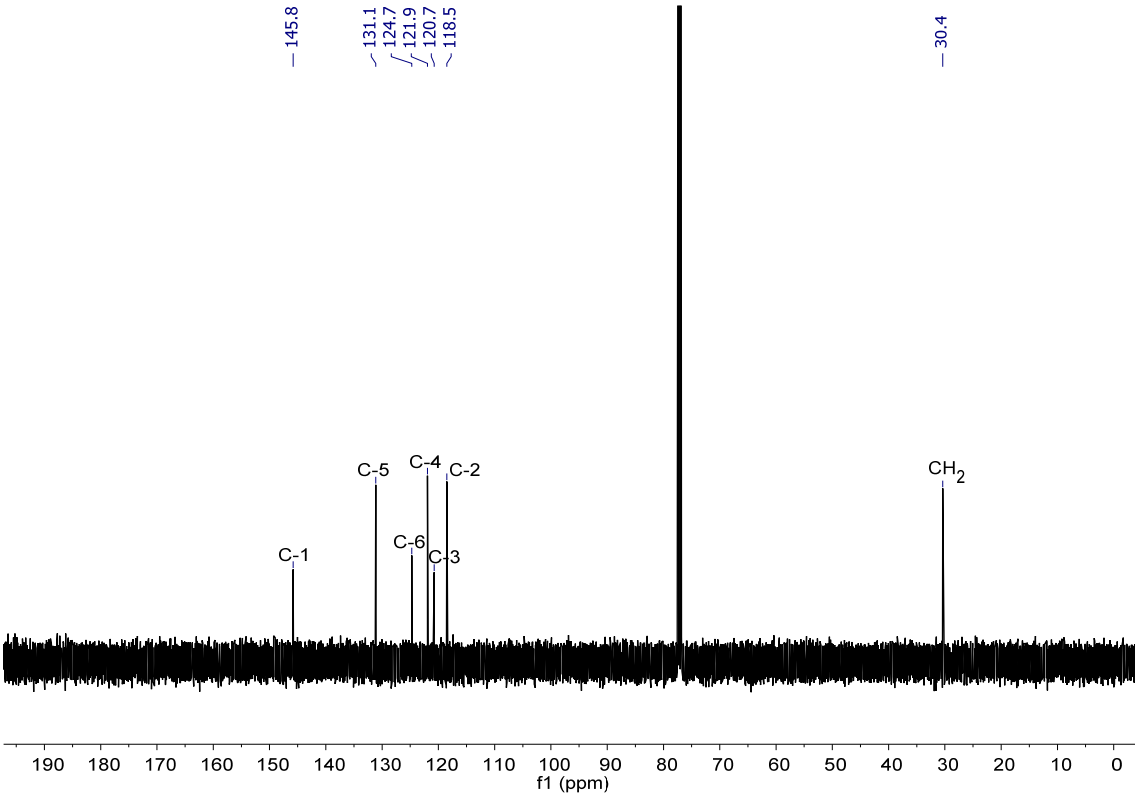

^{13}C NMR (125.8 MHz, $CDCl_3$)

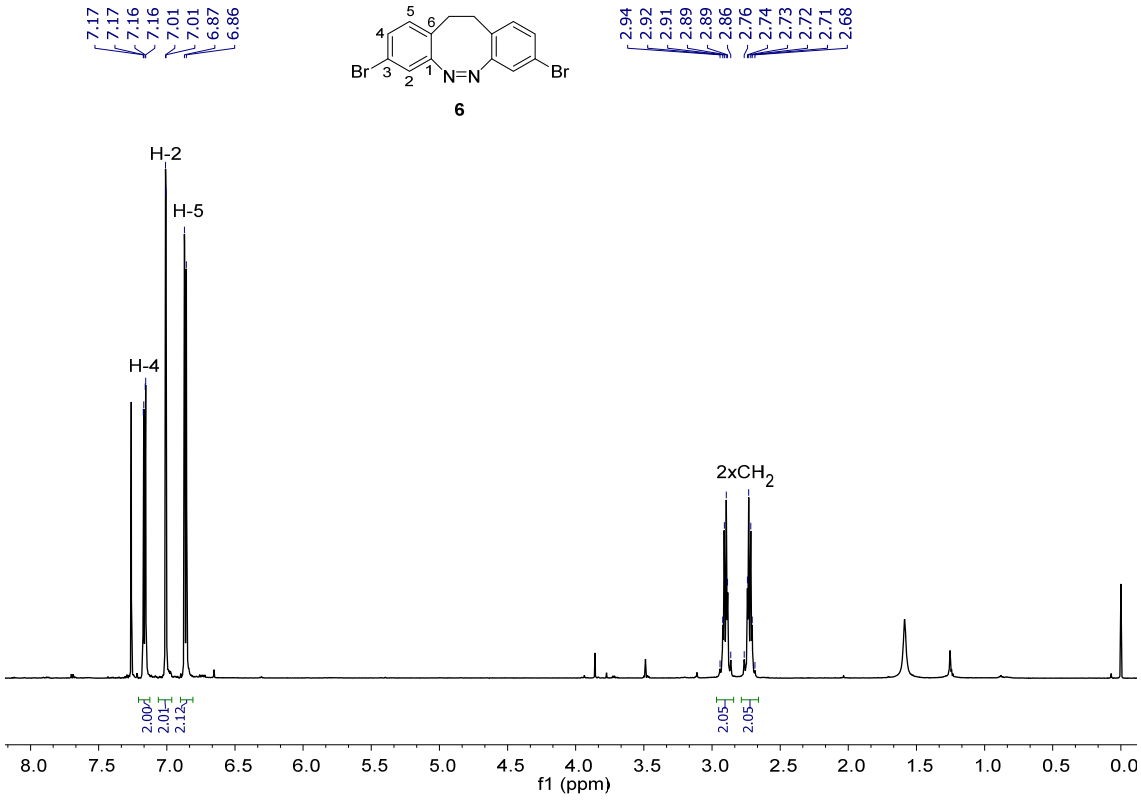

^{1}H NMR (500 MHz, $CDCl_3$)

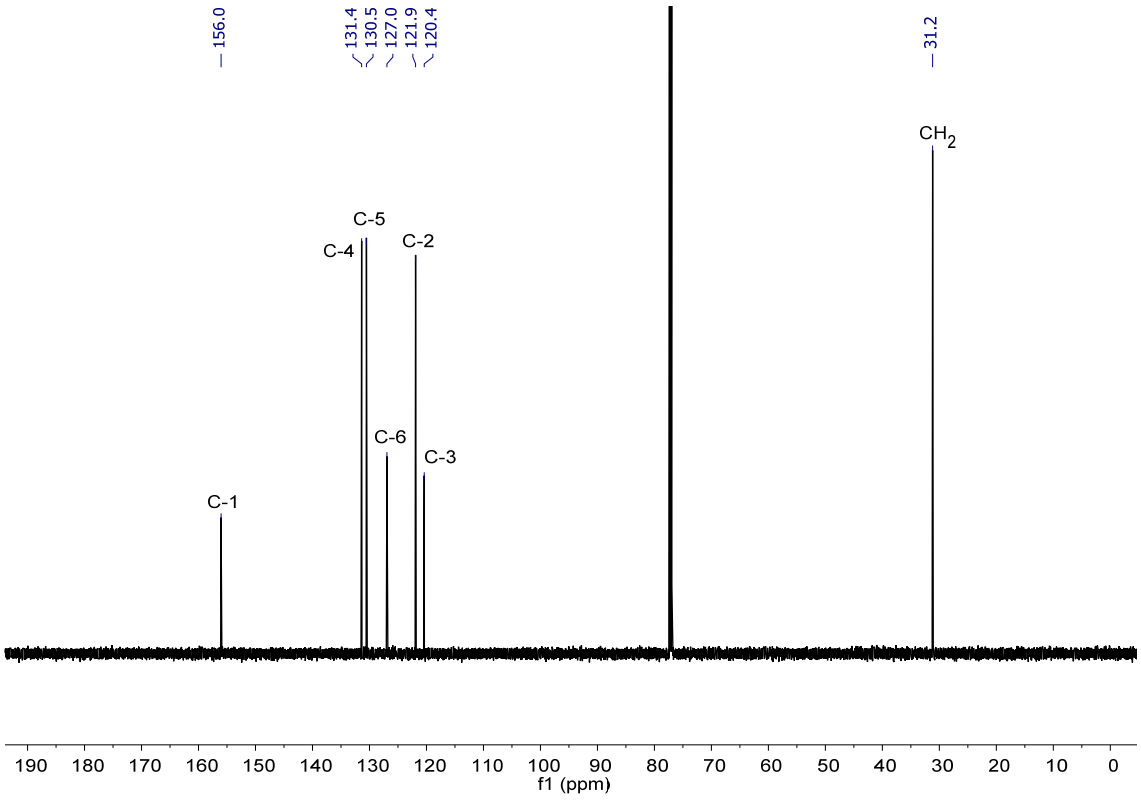

^{13}C NMR (125.8 MHz, $CDCl_3$)

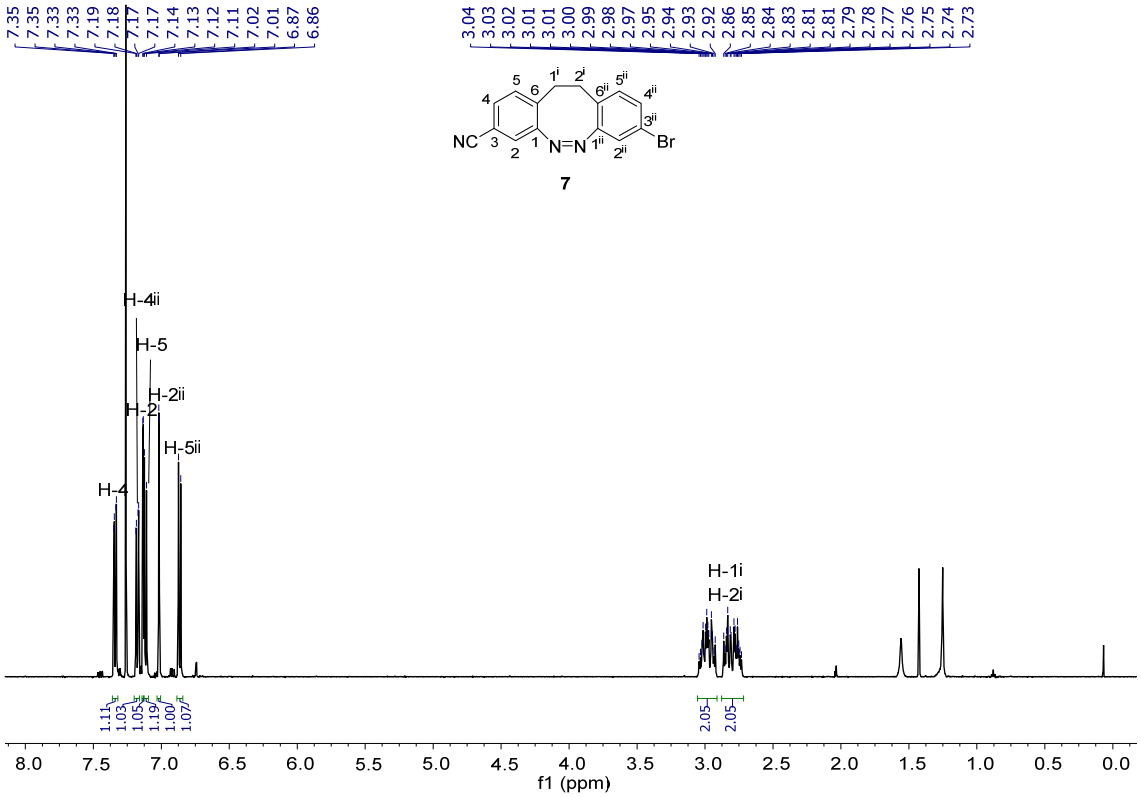

^{1}H NMR (500 MHz, $CDCl_3$)

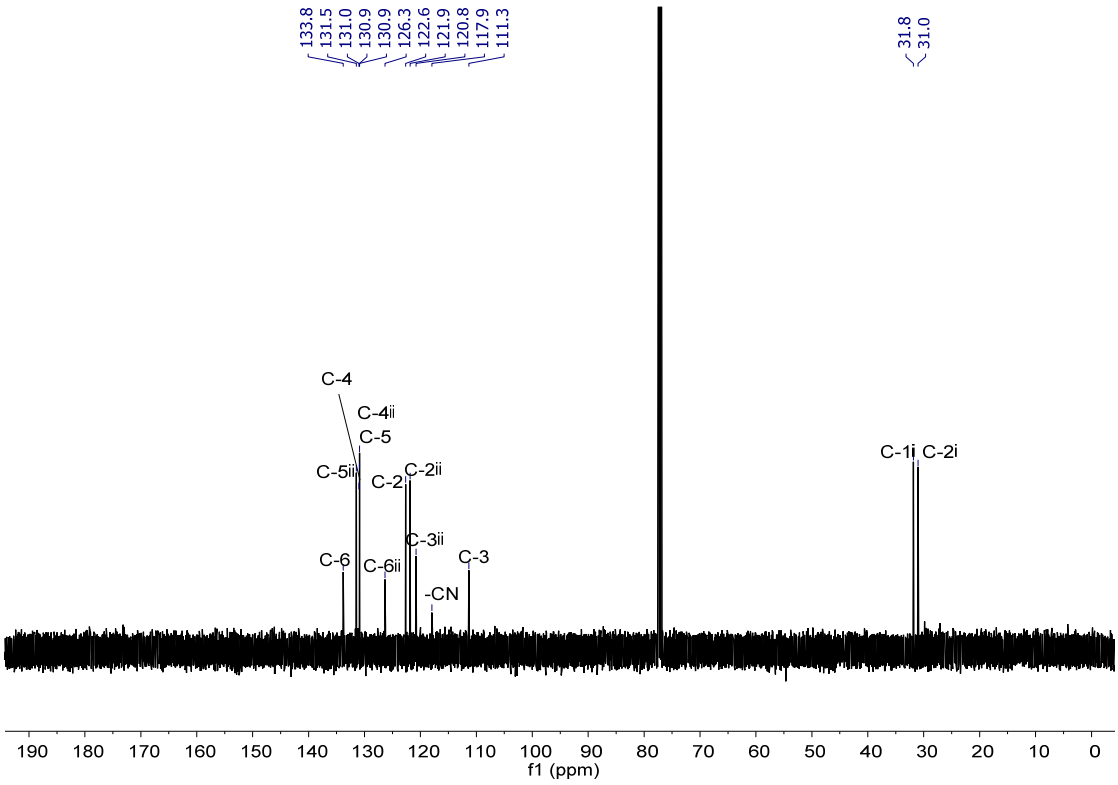

^{13}C NMR (125.8 MHz, $CDCl_3$)

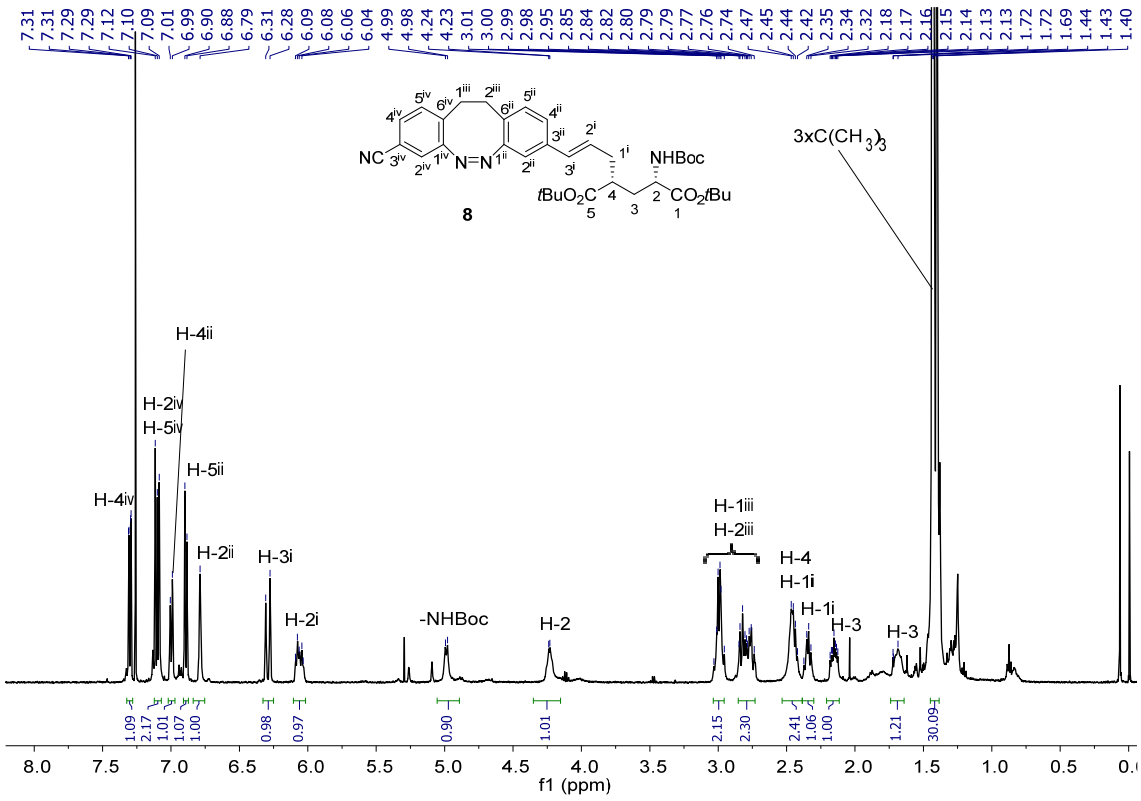

^{1}H NMR (500 MHz, $CDCl_3$)

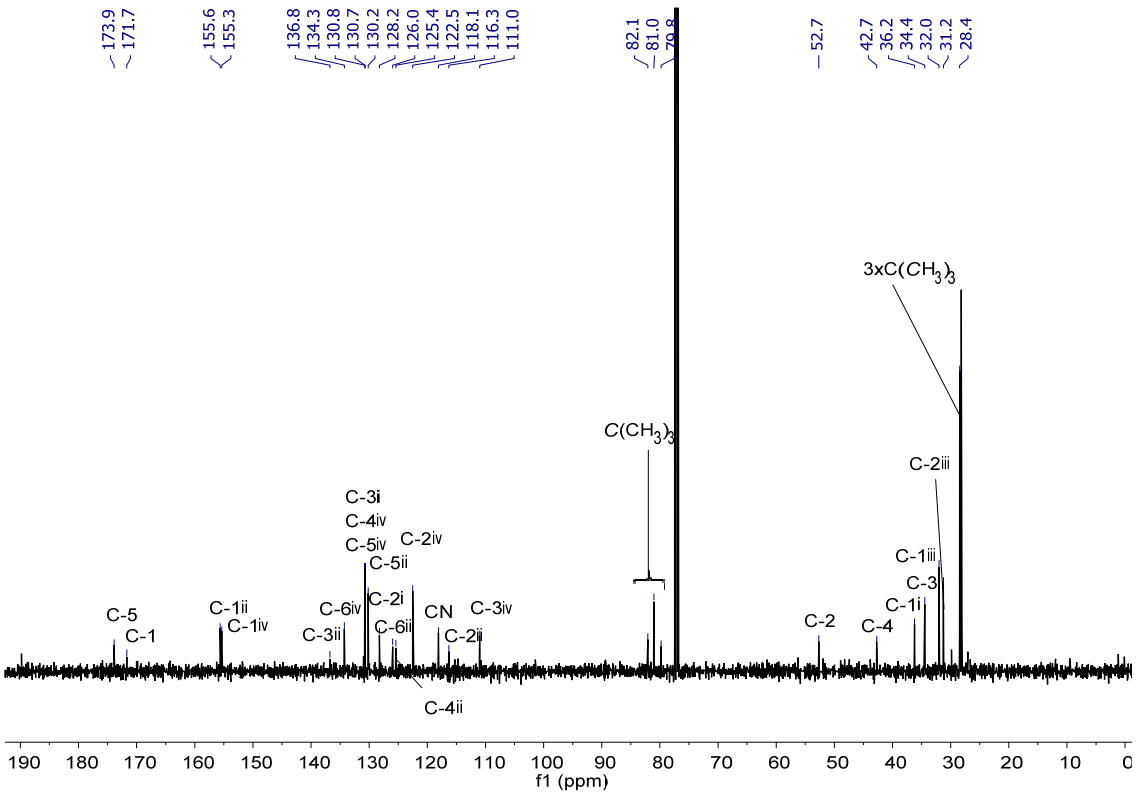

^{13}C NMR (125.8 MHz, $CDCl_3$)

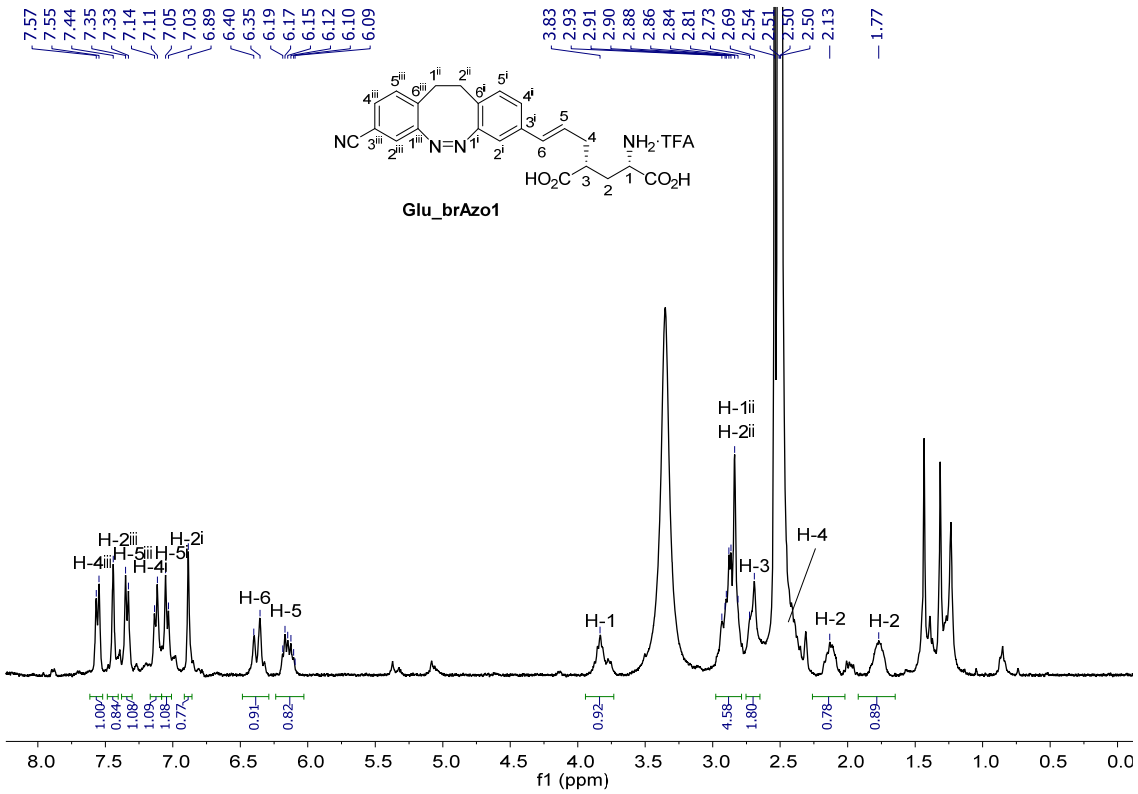

^{1}H NMR (360 MHz, DMSO-d_6)

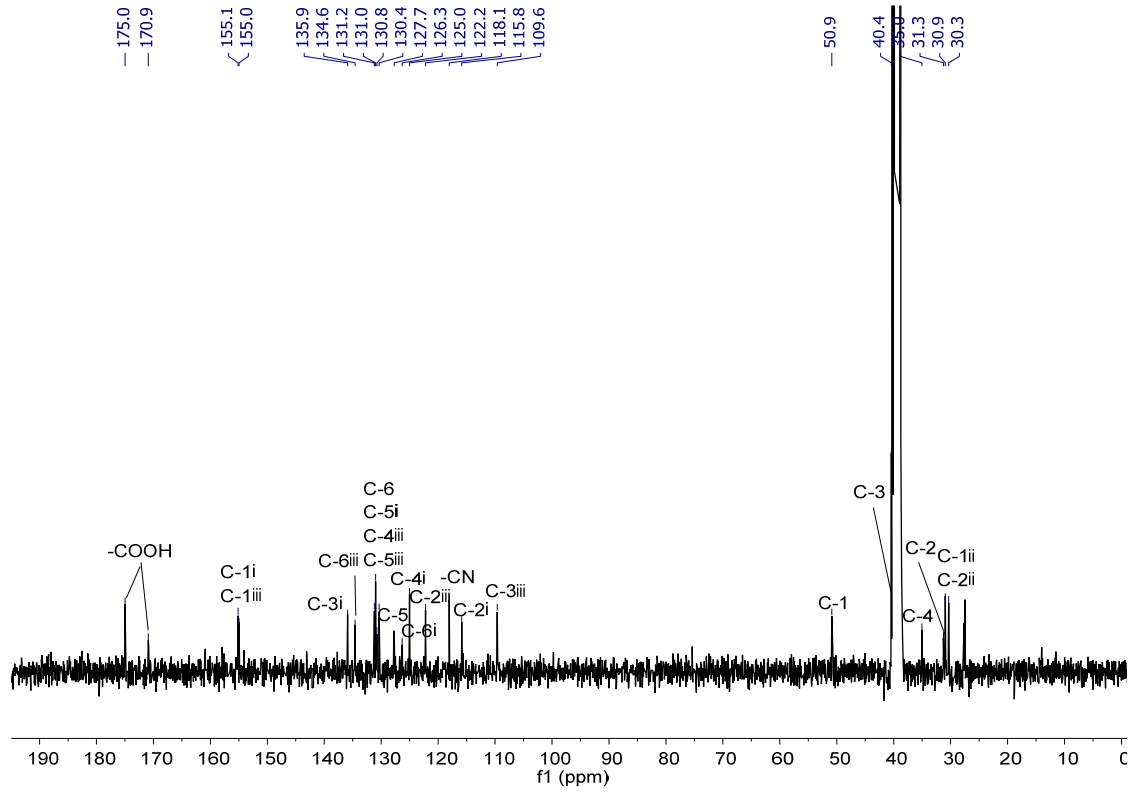

^{13}C NMR (90.5 MHz, DMSO-d_6)

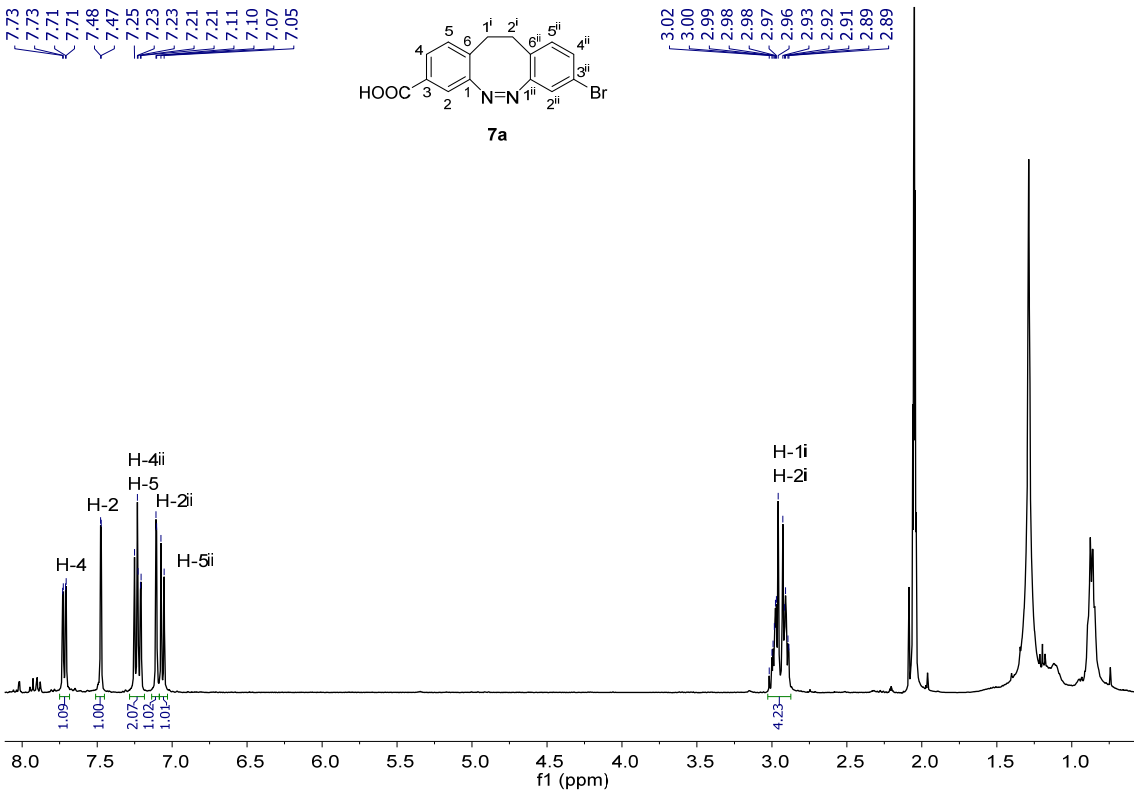

^{1}H NMR (400 MHz, acetone-d_6)

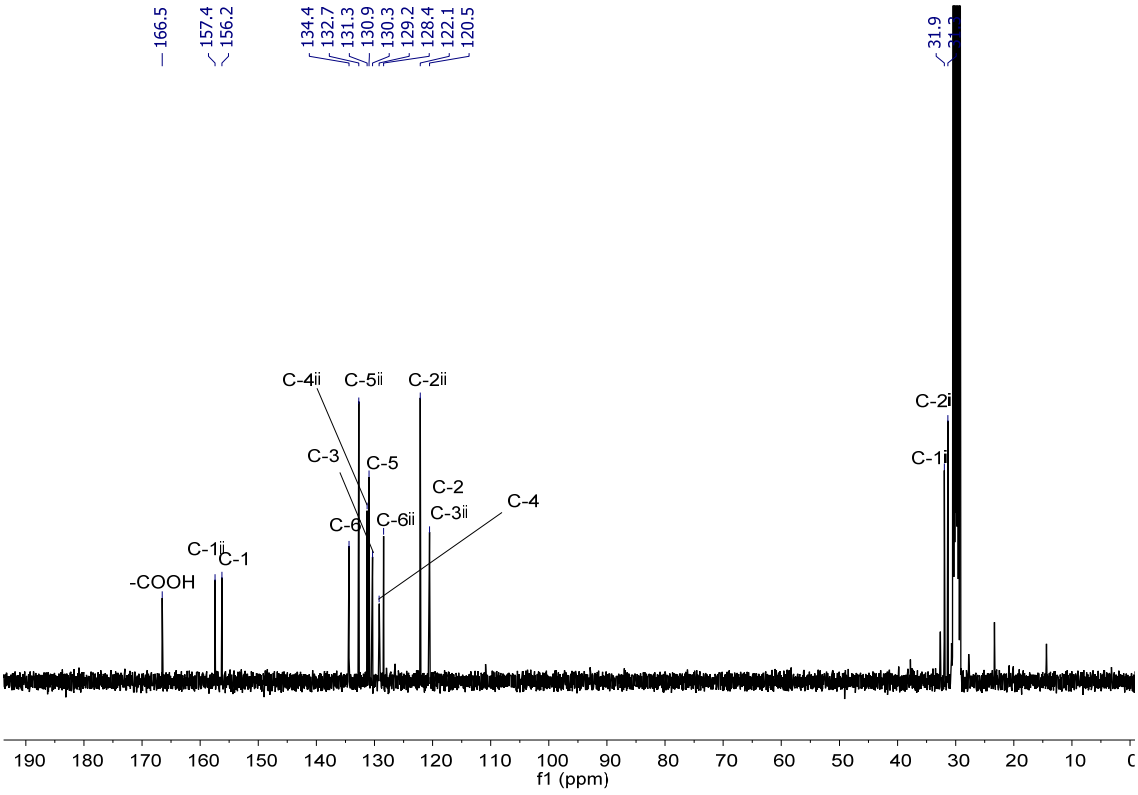

^{13}C NMR (100.6 MHz, acetone-d_6)

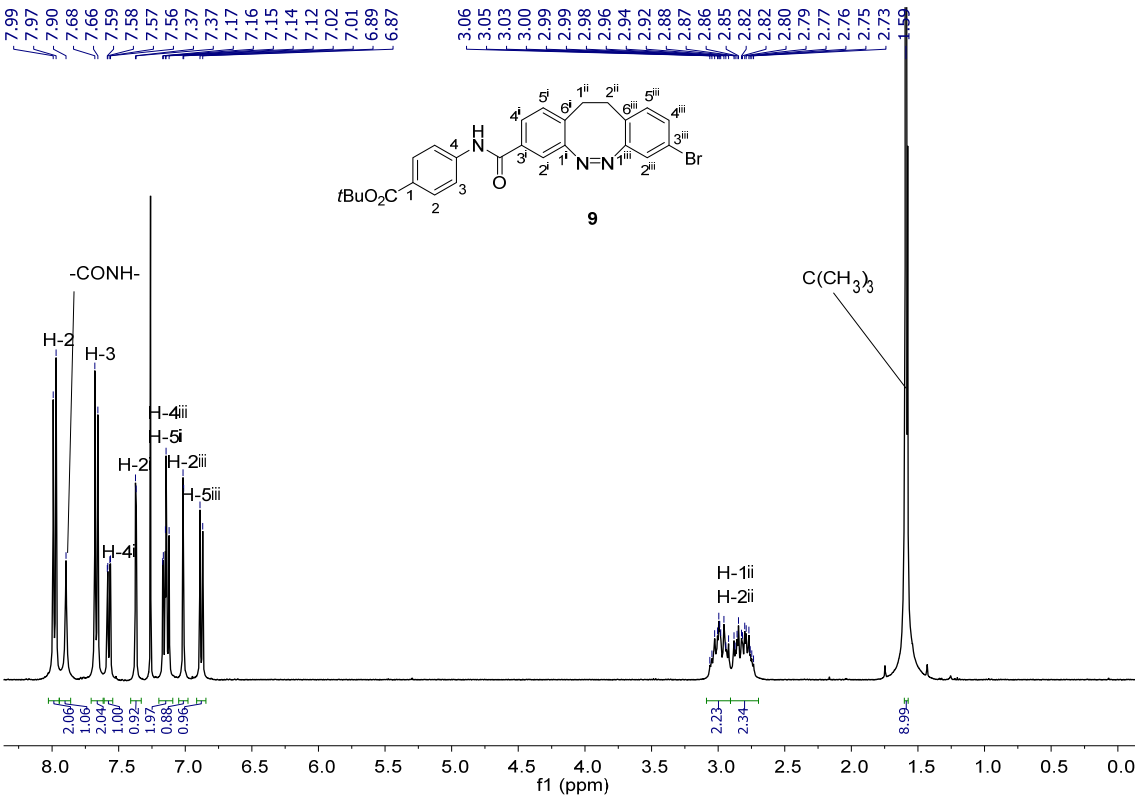

^{1}H NMR (400 MHz, $CDCl_3$)

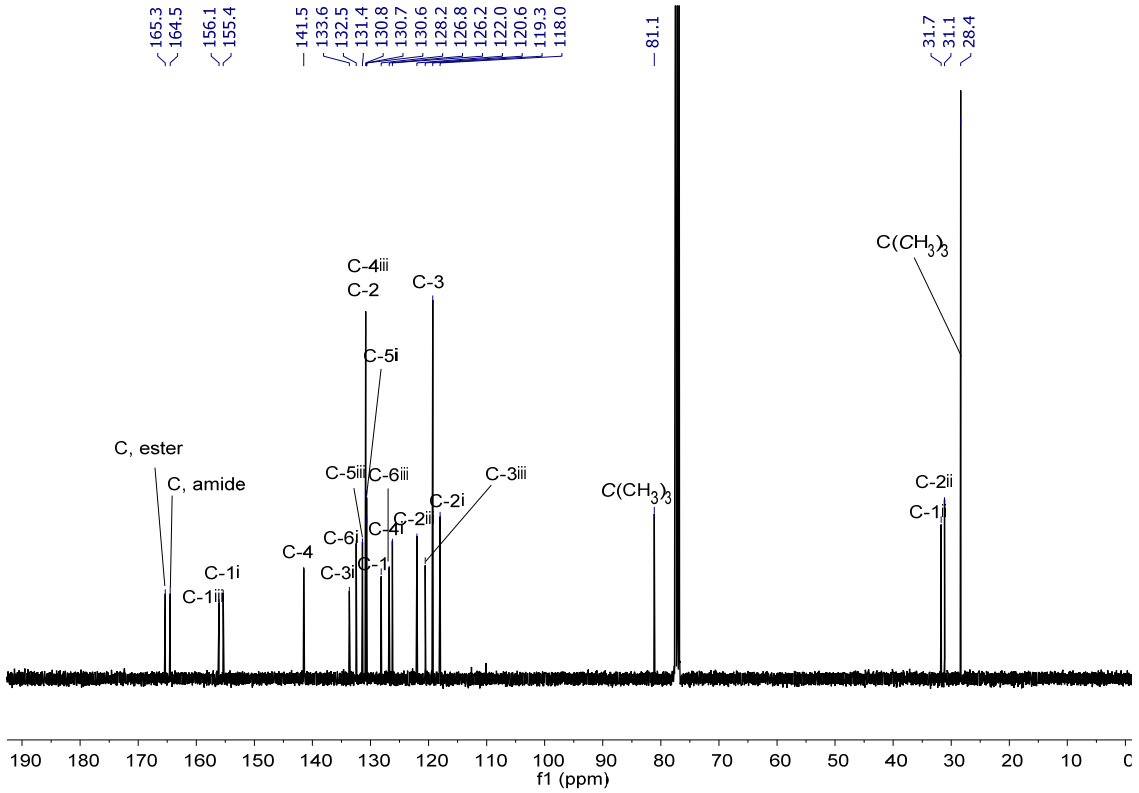

^{13}C NMR (100.6 MHz, $CDCl_3$)

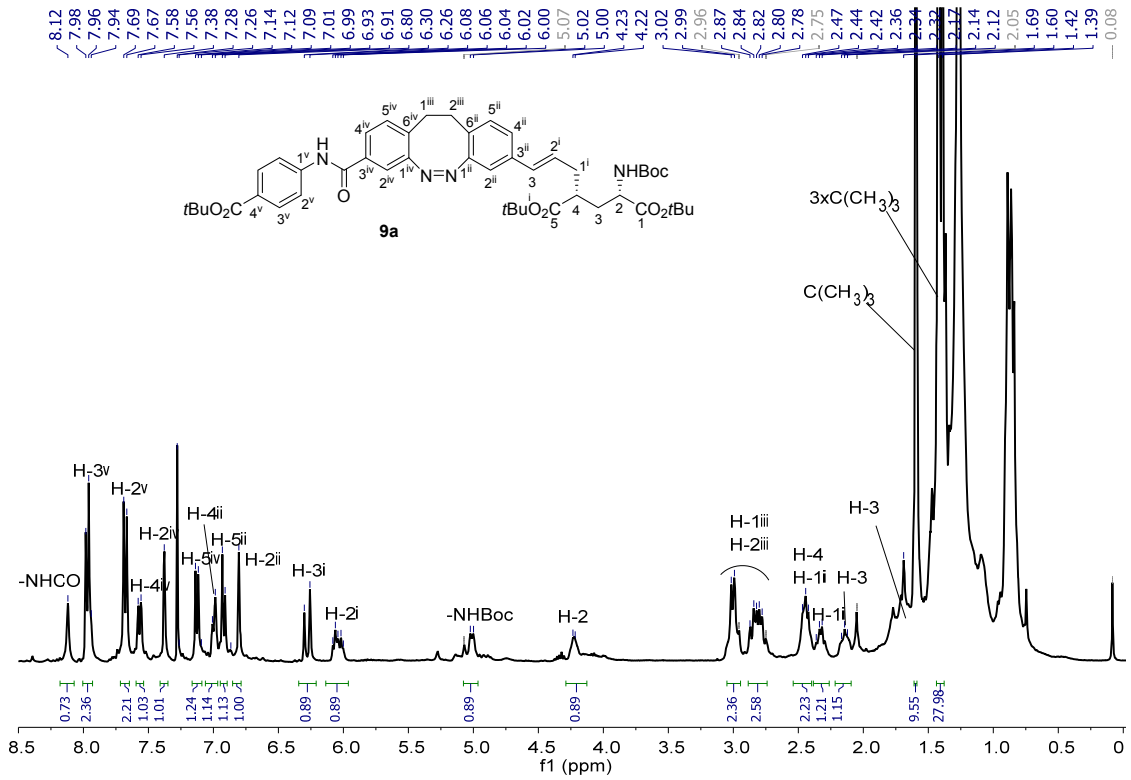

^{1}H NMR (360 MHz, $CDCl_3$)

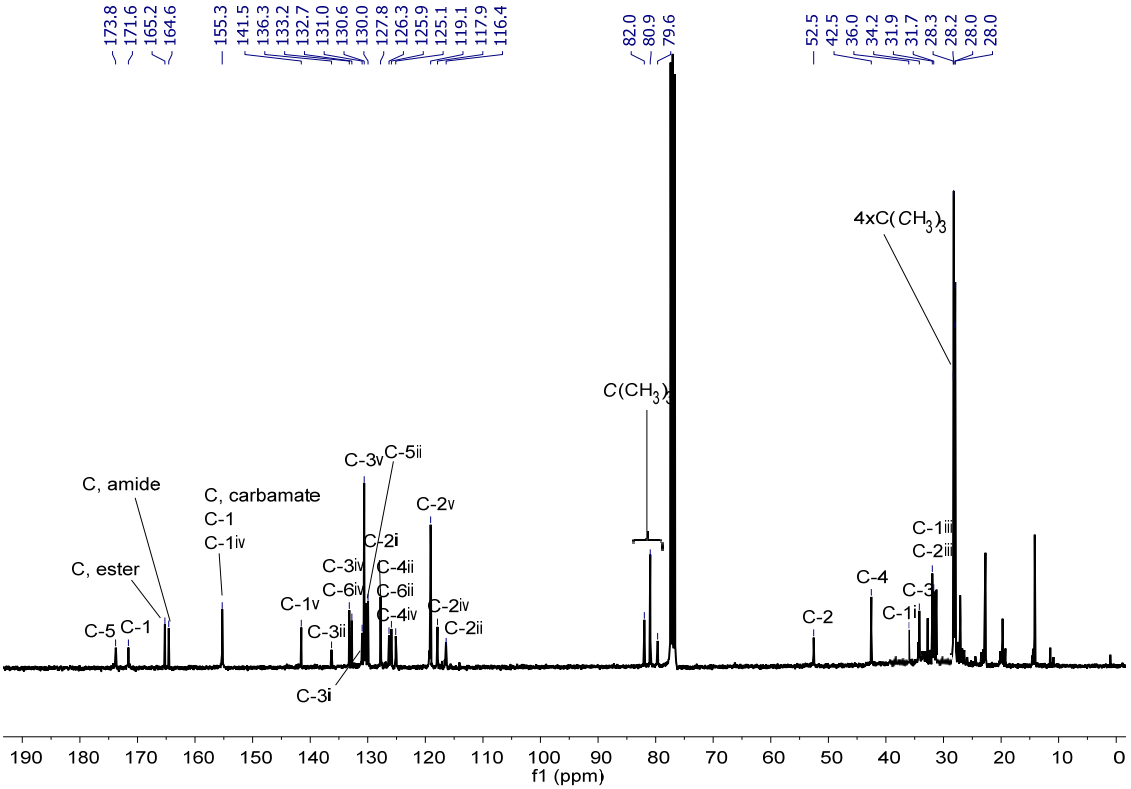

^{13}C NMR (90.6 MHz, $CDCl_3$)

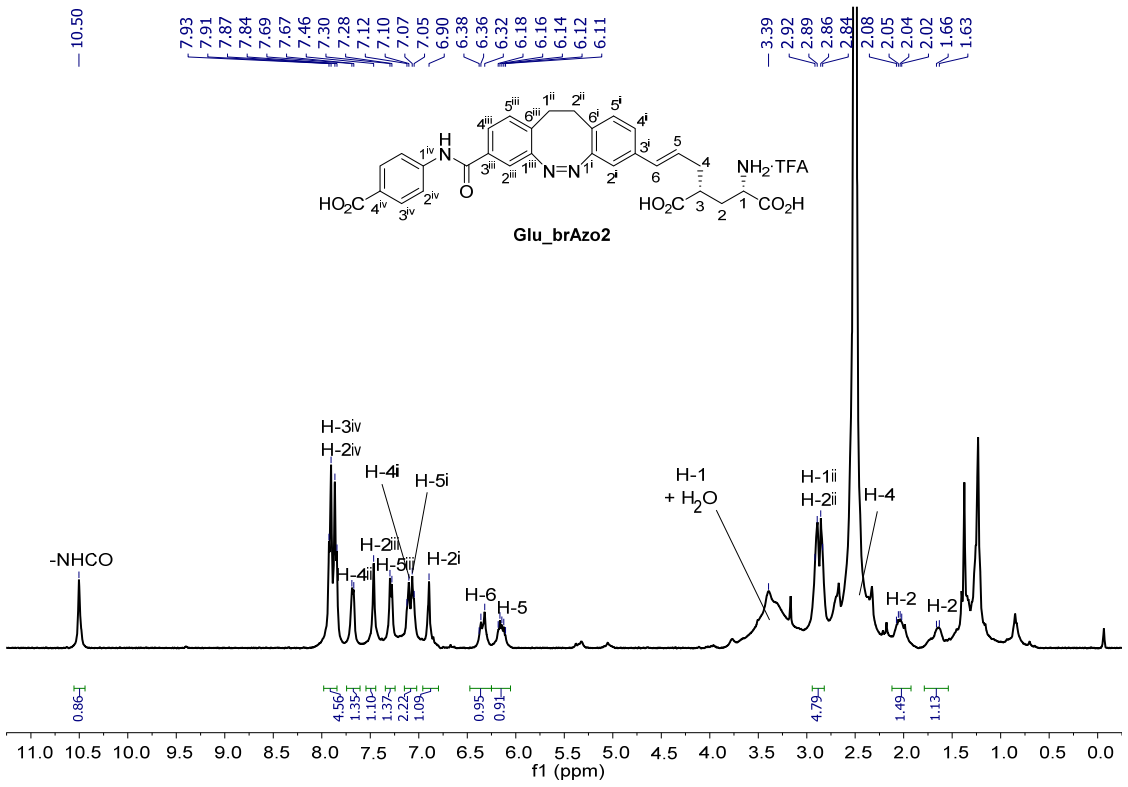

^{1}H NMR (400 MHz, DMSO-d_6)

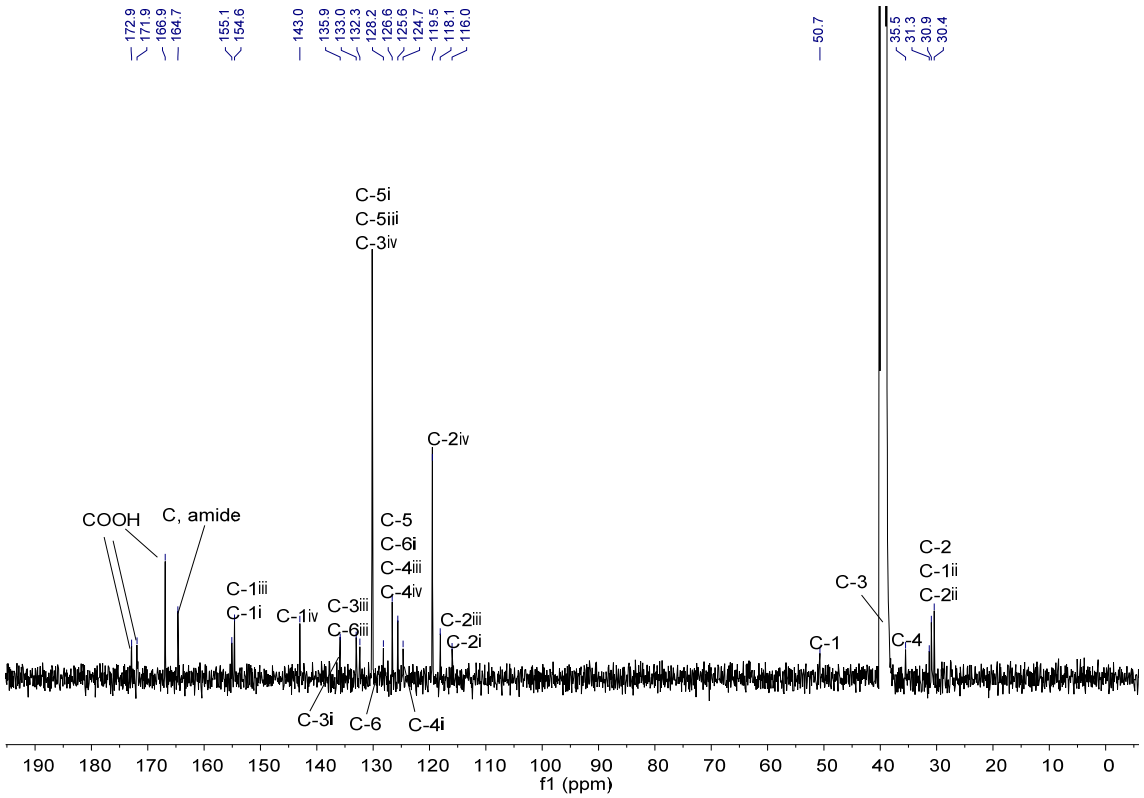

^{13}C NMR (90.6 MHz, DMSO-d_6)

References

[1] Gascón-Moya, M.; Pejoan, A.; Izquierdo-Serra, M.; Pittolo, S.; Cabré, G.; Hernando, J: Alibés, R.; Gorostiza, P.; Busqué, F. *J. Org. Chem.* **2015**, *80*, 9915-9925.

[2] Venkatachalam, T. K.; Huang, H.; Yu, G.; Uckun, F. M. *Synth. Commun.* **2004**, *34*, 1489-1497.

[3] Verdonk, M. L.; Cole, J. C.; Hartshorn, M. J.; Murray, C. W.; Taylor, R. D. *Proteins Struct. Funct. Biogenet.* **2003**, *52*, 609–623.

[4] Reiter, A.; Skerra, A.; Trauner, D.; Schiefner, A. *Biochemistry* **2013**, *52*, 8972-8974.

[5] Anandakrishnan, R.; Aguilar, B.; Onufriev, A. V. *Nucleic Acids Res.* **2012**, *40*, 537-541.

[6] GaussView, Version 6, Dennington, R.; Keith, T. A.; Millam, J. M. Semichem Inc., Shawnee Mission, KS, **2016**.

[7] Pettersen E. F.; Goddard, T. D.; Huang, C. C.; Couch, G. S.; Greenblatt, D. M.; Meng, E. C.; Ferrin, T. E. *J. Comput. Chem.* **2004**, *25*, 1605-1612.

[8] Gaussian 09, Revision C.01, Frisch, M. J.; Trucks, G. W.; Sch-legel, H. B.; Scuseria, G. E.; Robb, M. A.; et al. Gaussian, Inc., Wallingford CT, **2009**.

[9] Eldridge, M. D.; Murray, C. W.; Auton, T. R.; Paolini, G. V.; Mee, R. P. *J. Comput.-Aided Mol. Des.* **1997**, *11*, 425–445.

[10] Higashiguchi, K., Matsuda, K., Asano, Y.; Murakami, A.; Nakamura, S.; Irie, M. *Eur. J. Org. Chem*. **2005**, 91-97.

[11] Ren, Z.; Riley, N. J.; Needleman, L. A.; Sanders, J. M.; Swanson, G. T.; Marshall, J. *J. Biol. Chem*. **2003,** 278, 52700–52709.

[12] Halliwell, R. F.; Peters, J. A.; Lambert, J. J. *Br. J. Pharmacol.* **1989**, *96*, 480-494.

[13] Beaudoin, G. M.; Lee, S. H.; Singh, D.; Yuan, Y.; Ng, Y. G.; Reichardt, L. F.; Arikkath, J. *Nat. Protoc.* **2012**, *7*, 1741-1754.

[14] Kaech, S.; Banker; G. *Nat. Protoc.* **2006**, *1*, 2406-2415.